UNIVERSIDAD AUTONOMA DE AGUASCALIENTES

CENTRO DE CIENCIAS BÁSICAS

DEPARTAMENTO DE MATEMÁTICAS Y FÍSICA

TESIS

MATHEMATICAL MODEL OF THE EFFICIENCY OF A SILICON SOLAR CELL

PRESENTA

Héctor Alejandro Villalobos Martínez

PARA OPTAR POR EL GRADO DE MAESTRO EN CIENCIAS EN MATEMÁTICAS APLICADAS

COMITÉ TUTORAL

Dr. Jorge Eduardo Macías-Díaz (Co-tutor)
Dr. José Salvador Flores Hernández (Co-tutor)
Dra. Mariana Alfaro Gómez (Asesora)

Aguascalientes, Ags., 18 de febrero de 2021

UNIVERSIDAD AUTONOMA DE AGUASCALIENTES

FORMATO DE CARTA DE VOTO APROBATORIO

M. en C. Jorge Martín Alférez Chávez
DECANO DEL CENTRO DE CIENCIAS BÁSICAS
PRESENTE

Por medio de la presente, en mi calidad de co-tutor designado del estudiante **HÉCTOR ALEJANDRO VILLALOBOS MARTÍNEZ** con ID 141476 quien realizó la tesis titulada: **MATHEMATICAL MODEL OF THE EFFICIENCY OF A SILICON SOLAR CELL**, un trabajo propio, innovador, relevante e inédito y con fundamento en el Artículo 175, Apartado II del Reglamento General de Docencia doy mi consentimiento de que la versión final del documento ha sido revisada y las correcciones se han incorporado apropiadamente, por lo que me permito emitir el **VOTO APROBATORIO**, para que él pueda proceder a imprimirla, y así continuar con el procedimiento administrativo para la obtención del grado.

Pongo lo anterior a su digna consideración y, sin otro particular por el momento, me permito enviarle un cordial saludo.

ATENTAMENTE
"Se Lumen Proferre"
Aguascalientes, Ags., a 18 de febrero de 2021

Dr. Jorge Eduardo Macías-Díaz

c.c.p.- Interesado
c.c.p.- Secretaría de Investigación y Posgrado
c.c.p.- Consejero Académico
c.c.p.- Minuta Secretario Técnico

UNIVERSIDAD AUTONOMA DE AGUASCALIENTES

FORMATO DE CARTA DE VOTO APROBATORIO

M. en C. Jorge Martín Alférez Chávez
DECANO DEL CENTRO DE CIENCIAS BÁSICAS
PRESENTE

Por medio de la presente, en mi calidad de cotutor designado del estudiante **HÉCTOR ALEJANDRO VILLALOBOS MARTÍNEZ** con ID 141476 quien realizó la tesis titulada: **MATHEMATICAL MODEL OF THE EFFICIENCY OF A SILICON SOLAR CELL**, un trabajo propio, innovador, relevante e inédito y con fundamento en el Artículo 175, Apartado II del Reglamento General de Docencia doy mi consentimiento de que la versión final del documento ha sido revisada y las correcciones se han incorporado apropiadamente, por lo que me permito emitir el **VOTO APROBATORIO**, para que él pueda proceder a imprimirla, y así continuar con el procedimiento administrativo para la obtención del grado.

Pongo lo anterior a su digna consideración y, sin otro particular por el momento, me permito enviarle un cordial saludo.

ATENTAMENTE
"Se Lumen Proferre"
Aguascalientes, Ags., a 18 de febrero de 2021

Dr. José Salvador Flores Hernández

c.c.p.- Interesado
c.c.p.- Secretaría de Investigación y Posgrado
c.c.p.- Consejero Académico
c.c.p.- Minuta Secretario Técnico

UNIVERSIDAD AUTÓNOMA DE AGUASCALIENTES

FORMATO DE CARTA DE VOTO APROBATORIO

M. en C. Jorge Martín Alférez Chávez
DECANO DEL CENTRO DE CIENCIAS BÁSICAS
PRESENTE

Por medio de la presente, en mi calidad de asesor designado del estudiante **HÉCTOR ALEJANDRO VILLALOBOS MARTÍNEZ** con ID 141476 quien realizó la tesis titulada: **MATHEMATICAL MODEL OF THE EFFICIENCY OF A SILICON SOLAR CELL**, un trabajo propio, innovador, relevante e inédito y con fundamento en el Artículo 175, Apartado II del Reglamento General de Docencia doy mi consentimiento de que la versión final del documento ha sido revisada y las correcciones se han incorporado apropiadamente, por lo que me permito emitir el **VOTO APROBATORIO**, para que él pueda proceder a imprimirla, y así continuar con el procedimiento administrativo para la obtención del grado.

Pongo lo anterior a su digna consideración y, sin otro particular por el momento, me permito enviarle un cordial saludo.

ATENTAMENTE
"Se Lumen Proferre"
Aguascalientes, Ags., a 18 de febrero de 2021

Dra. Mariana Alfaro Gómez

c.c.p.- Interesado
c.c.p.- Secretaría de Investigación y Posgrado
c.c.p.- Consejero Académico
c.c.p.- Minuta Secretario Técnico

DICTAMEN DE LIBERACIÓN ACADÉMICA PARA INICIAR LOS TRÁMITES DEL EXAMEN DE GRADO

Fecha de dictaminación dd/mm/aaaa: 2/18/2021

NOMBRE: Héctor Alejandro Villalobos Martínez **ID** 141476

PROGRAMA Maestría en Ciencias con opción en Matemáticas Aplicadas **LGAC (del posgrado):** Matemáticas Aplicadas

TIPO DE TRABAJO: (x) Tesis ( ) Trabajo Práctico

TITULO: Mathematical model of the efficiency of a silicon solar cell

IMPACTO SOCIAL (señalar el impacto logrado

Impacto en la generación de conocimiento científico.

INDICAR SI NO N.A. (NO APLICA) SEGÚN CORRESPONDA:

Elementos para la revisión académica del trabajo de tesis o trabajo práctico:	
SI	El trabajo es congruente con las LGAC del programa de posgrado
SI	La problemática fue abordada desde un enfoque multidisciplinario
SI	Existe coherencia, continuidad y orden lógico del tema central con cada apartado
SI	Los resultados del trabajo dan respuesta a las preguntas de investigación o a la problemática que aborda
SI	Los resultados presentados en el trabajo son de gran relevancia científica, tecnologíca o profesional según el área
SI	El trabajo demuestra más de una aportación original al conocimiento de su área
NO	Las aportaciones responden a los problemas prioritarios del país
NO	Generó transferecia del conocimiento o tecnológica
N.A.	Cumple con la ética para la investigación (reporte de la herramienta antiplagio)
El egresado cumple con lo siguiente:	
SI	Cumple con lo señalado por el Reglamento General de Docencia
SI	Cumple con los requisitos señalados en el plan de estudios (créditos curriculares, optativos, actividades complementarias,estancia, predoctoral, etc)
SI	Cuenta con los votos aprobatorios del comité tutoral, en caso de los posgrados profesionales si tiene solo tutorpodrá liberar solo el tutor
N.A.	Cuenta con la carta de satisfacción del Usuario
SI	Coincide con el título y objetivo registrado
SI	Tiene congruencia con cuerpos académicos
SI	Tiene el CVU del Conacyt actualizado
N.A.	Tiene el artículo aceptado o publicado y cumple con los requisitos institucionales (en caso que proceda)
En caso de Tesis por artículos científicos publicados	
N.A.	Aceptación o Publicación de los articulos según el nivel del programa
N.A.	El estudiante es el primer autor
N.A.	El autor de correspondencia es el Tutor del Núcleo Académico Básico
N.A.	En los artículos se ven reflejados los objetivos de la tesis, ya que son producto de este trabajo de investigación.
N.A.	Los artículos integran los capítulos de la tesis y se presentan en el idioma en que fueron publicados
N.A.	La aceptación o publicación de los artículos en revistas indexadas de alto impacto

Con base a estos criterios, se autoriza se continúen con los trámites de titulación y programación del examen de grado: **Sí** _____

_____

FIRMAS

Elaboró:

* NOMBRE Y FIRMA DEL CONSEJERO SEGÚN LA LGAC DE ADSCRIPCION: Jorge Eduardo Macías Díaz

NOMBRE Y FIRMA DEL SECRETARIO TÉCNICO:

*** En caso de conflicto de intereses, firmará un revisor miembro del NAB de la LGAC correspondiente distinto al tutor o miembro del comité tutoral, asignado por el Decano**

Revisó:

NOMBRE Y FIRMA DEL SECRETARIO DE INVESTIGACIÓN Y POSGRADO: DRA. HAYDEE MARTÍNEZ RUVALCABA

Autorizó:

NOMBRE Y FIRMA DEL DECANO:

Nota: procede el trámite para el Depto. de Apoyo al Posgrado

En cumplimiento con el Art. 105C del Reglamento General de Docencia que a la letra señala entre las funciones del Consejo Académico: .... Cuidar la eficiencia terminal del programa de posgrado y el Art. 105F las funciones del Secretario Técnico, llevar el seguimiento de los alumnos.

Acknowledgments

Firstly, I want to thank to CONACYT and UAA for the economical support that enable me to course the Master's degree.

I also want to thank all the help and patience of all my teachers and advisors who showed me a new way to see mathematics as an engineer.

This thesis would not be possible without the support of my wife, Jacqueline, who had my back since day one and always encourage me to be better.

And, last but not least, thanks to my family for all the help, for raising me as curious man and teaching me to always aspire for the best.

Héctor Alejandro Villalobos Martínez

Contents

List of Tables

List of Figures

Resumen

Este trabajo está dedicado a la modelación de una celda solar de silicio con el fin de mejorar su eficiencia, está basado en las ecuaciones de continuidad, transporte y Poisson para modelar el comportamiento de los portadores de carga en un semiconductor.

Se estudió cuidadosament el fenómeno fotovoltaico en las células solares de silicio para desarrollar el modelo e identificar aquellos parámetros que juegan un papel crucial en los valores que determinan su eficiencia. Estos parámetros incluyen los coeficientes de difusión, movilidad y absorción, la permitividad, el ancho de las regiones y la vida útil de los portadores minoritarios.

El modelo de celda solar es un sistema de ecuaciones diferenciales parciales elípticas-parabólicas quasi-lineales de segundo orden con acoplamiento fuerte e interfaz, modelado sobre un dominio compuesto por tres regiones con diferentes propiedades eléctricas.

A pesar de que existen modelos de células solares preexistentes, hasta donde sabemos, no existen teoremas de existencia y unicidad con los que trabajar. Sobre dichos modelos , se realizan diferentes supuestos con el fin simplificarlos para poder resolverlos, principalmente, mediante métodos numéricos.

A lo largo de este trabajo se presentan los fundamentos físicos del efecto fotovoltaico con el fin de ayudar al lector a comprender el desarrollo del modelo y sus condiciones, una vez presentado el modelo, se realiza un análisis cualitativo para identificar el comportamiento que los parámetros deben tener en el modelo, para posteriormente se compararlo con la literatura para demostrar su singularidad y relevancia.

Abstract

This dissertation is devoted to model a silicon solar cell in order to enhance its efficiency, this is formulated based on the continuity, transport and Poisson equations to model the behavior of charge carriers in a semiconductor.

The photovoltaic phenomenon on silicon solar cells was carefully studied to develop the model and identify those parameters that play a crucial roll in its efficiency values. This parameters include the diffusion, mobility and absorption coefficients, the permittivity, the regions width and the minority carrier lifetime.

The solar cell model is a quasi-linear second order elliptic-parabolic partial differential equation system with strong coupling and interface, modeled over a domain composed of three regions with different electrical properties.

As far as we know, there are not existence and uniqueness theorems to work with even though there are preexisting solar cell models. On this preexisting models, different assumptions to simplify them are done in order to be able to solve them, mostly, using numerical methods.

Along this dissertation, the fundamental physics of the photovoltaic effect are presented in order to help the reader to understand the development of the model and its conditions, after the model is presented, a qualitative analysis is made to identify the behavior that the parameters must have in the model, then the model is compared with those in the literature to demonstrate its uniqueness and relevance.

Introduction

The constant growth in the world population, combined with the current lifestyle, has generated an increase in the energy consumption. This is reflected in the fact that world population grew a 44% [1] while the energy consumption a 63% [2] from 1990 to 2018.

In the last years, the renewable energies have received great interest due to their high availability, low pollution rates and maintenance costs. They represented 25% of the world electric energy generation in 2017, where we can highlight wind power, biomass and solar which had a growth of the 186, 35 and 1033 % respectively, from 2010 and 2017 [3].

The growth exhibited by the solar energy is no surprise since the Sun radiates 62 MW/m^2 [4], which is ten thousand times bigger than the daily world energy consumption [5], additionally its technologies, thermosolar and photovoltaic, have a simple installation and ease to modify the installed power according to the needs. Photovoltaic technologies turn solar radiation directly into electricity based on the use of solar cells i.e. thin films and crystalline silicon (c-Si) structures. This last one is most mature because of its high availability, no toxicity, low cost and cell manufacturing capacity with high and stable conversion efficiency [6]. Si technologies represent more than the 80% of sold photovoltaic modules in the world and is subdivided, depending on the kind of used Si, in: monocrystalline, policrystalline, amorphous and hybrid [7].

The efficiency of Si solar cells is given in terms of the output power and the incident radiation per area unit, hence to reduce the area occupied by the cell is important to maximize the efficiency.

The theoretical limit of a c-Si cell under non-concentrated solar light is around 29% which has not been reached, the best laboratory silicon solar cell has an efficiency over the 24% and is manufactured by SunPower [6].

To increase this efficiency, research about alternative manufacturing approaches in combination with fine wafers, low optical gain, band-gap engineering for a better optical absorption [8], selective passivation contacts [9], temperature control [10] and advanced solar cells configurations [11] is being developed [13, 14]. The previous cited researches have been carried out experimentally which can be very expensive.

The use of mathematical models aided by computational tools have been developed to reduce experimentation costs; the most basic models of these technologies are those based on equivalent circuits as those presented in [15, 16, 17, 18]. Also some simulations and calculations are made to vary the operation parameters of a solar cell such as temperature and irradiation levels [19, 20, 21,

22], characteristics of the interconnection ribbons [23, 24], impact of dust over the cell surface [25], solar tracking systems [26], surface texturing [27] and partial shadowing [28] in order to obtain the performance curves and compare them with real solar cells.

PC1D is a software which is able to solve the fully coupled nonlinear equations for the quasi-one-dimensional transport of electrons and holes in photovoltaic cells, this software allows to vary the main parameters of the construction and operation of a solar cell. Based on this software, Basore presents and solves the physical and numerical models that make possible to approximate the multidimensional effects found in textured crystalline silicon solar cells [29].

More specialized and specific projects have been developed based on partial differential equations using the Poisson and Boltzmann Transport Equations, this last one is a complex equation which can explain the behavior of microscopic particles in semiconductor devices which has been solved using different tools such the Galerkin method [19], linear approximation and domain decomposition [30], and a WENO (weighted essentially non-oscillatory) solver [31].

Due the complexity of the Boltzmann Transport Equation, it is often used in its macroscopic forms which are known as the drift-diffusion model, used by Foster for the modeling of a Perovskite solar cell [67] and Kirchartz to model organic solar cells [33] both in steady state, and the hydrodynamic model, used to modeling of a GaAs solar cell [34].

On the other hand, the challenges to simulate a solar cell are to determinate the mobility and the recombination/generation rate [33, 35] and to properly model the parameters such as the intrinsic carrier density [36] and the diffusion length [37].

The Poisson and drift-diffusion equations can be solved in different ways depending on the established conditions, for example numerically discretizing using Scharfetter-Gummel and solving by Gummel iteration method [38] or discretizing by standard finite difference method in space and time to solve both the time-dependent and stationary problems using Gummel-Schwarz double iteration, a classical upwind discretization of the advection for the space variable for stability of the system, and the forward Euler scheme for the time variable [41]; while analytically solutions have been obtained using constant field method/single exponential approximation [35] and Riccati substitution [42], this analytical solutions have only been obtained by making not so real world assumptions or in steady state.

Accordingly, the boundary behavior is very important to solve the equations since different possible types of boundary conditions can be established depending on the type of metallic contacts on the semiconductor [41] and in the case of numerical solutions the mesh must fulfill different conditions [36, 43].

In order to solve mathematically correct this kind of equations, theorems to prove existence, uniqueness, regularity and asymptotic behavior of the solutions must be used as [44] does when modeling a semiconductor device defining a specific domain with its boundary conditions and as [45] where they establish the characteristics that the reaction and diffusion function must satisfy in a quasilinear parabolic–elliptic chemotaxis system in order to ensure a unique global classical solution which is a similar work as presented in [46, 47] with the difference that [46] includes theorems for weak solutions and asymptotic behavior. In [33] is mentioned that a finite difference method is an usual way to obtain the solution of the system with a Scharfetter–Gummel method to have a numerically stable solver which they recommend to be used only for the first iterations and then switch to

the fully coupled method for the rest to get better convergence.

The previous mentioned researches open the path for us to develop our model and enrich the existing mathematical models and experimental works since most of these references treat the problem in a similar way than us but in a steady state or for a solar technology different from silicon, which motivate us to develop a time transcendent model for silicon since it is the most common technology for solar cells, this formulation generates a parabolic-elliptic differential equation system therefore all the mathematical theory will be focused on this type of problems.

Consequently, we are interested in developing a mathematical and computational model that allows us to study, understand and predict the behavior of a solar cell efficiency to contribute in their improvement. By developing this model we can vary the different parameters that affect its efficiency in order to maximize it. Also, counting with a tool like this for the most basic solar technology can help to develop the new technologies since they have (practically) the same operating principle.

Objectives

General objective

- To develop and validate a mathematical model that improves the efficiency of silicon solar cells.

Specific objectives

- To obtain a mathematical model which determines the efficiency of a solar cell involving the most relevant phenomenons and experimental factors of the photovoltaic effect.
- To qualitatively analyze the obtained model demonstrating existence, uniqueness and asymptotic behavior of the solution.
- To implement a numeric method to approximate solutions of the continuous model.
- To computationally simulate the model modifying the studied experimental factors and comparing it with experimental results.
- To adjust the model parameters to approximate more efficiently the photovoltaic effect.

1. Solar cell physics

In this chapter we analyze the photovoltaic effect in order to understand how solar energy is transformed into electrical energy in a solar cell. In Section 1.1, we first introduce the concept of charge carriers in a semiconductor then explain the doping process and finally present the physics involved in a P-N junction. In Section 1.2, we address the photovoltaic effect by studying how certain factors in the P-N junction facilitate or limit the recombination and generation of charge carriers when a flow of photons produced by solar rays is absorbed in a solar cell.

1.1 Semiconductors: Generalities and properties

To get a better understanding of the working of a solar cell, in this section we study the structure and properties of its main component, silicon (Si), a semiconductor very abundant in the Earth. Electrical properties in the solids are determined by the distribution of the electrons in the valence and conduction bands, see Figure 1.1.

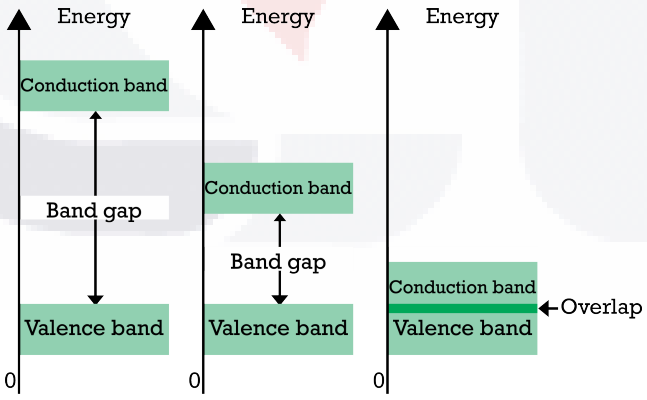

Figure 1.1: Band diagram for insulators(left), semiconductors (center) and conductors (right).

In conductors, the conduction and valence band are overlaped allowing an easy movement of the electrons between the bands. Meanwhile, electrons in the valence band of semiconductors and insulators need a certain amount of energy to jump to the conduction band, lower than 5 eV for semiconductors and higher than 5 eV for insulators, this energy is known as energy gap or band gap

and is denoted by E_g.

Electrons in a semiconductor are arranged in a crystalline structure, particularly, the atoms in Si share its valence electrons creating covalent bonds. This way, as we can see in Figure 1.2, there are not free electrons (at absolute zero) that can move between bands. However, if certain amount of energy is applied, as example an increment of temperature, an electron will acquire enough energy to break a bond and convert itself in a free electron and to create a hole (positively charged specie), in a semiconductor the electron and hole are known as charge carriers.

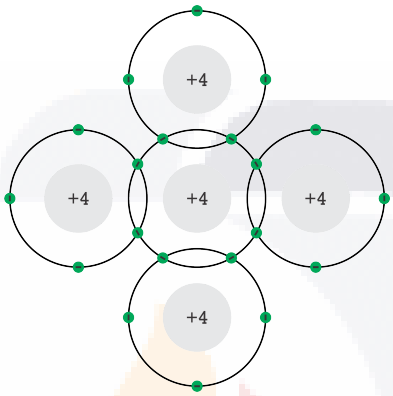

Figure 1.2: Crystalline structure between five atoms of silicon.

1.1.1 Semiconductor Doping

The process of adding atoms of other materials (impurities) in the atomic structure of a semiconductor in order to modify its properties is called doping; a semiconductor is named intrinsic when it is pure and extrinsic when it is doped.

When a certain amount of atoms elements of V-A group are added to Si, as it is shown in Figure 1.3 with phosphorus atoms, the impurity atoms form covalent bonds with silicon atoms, but since the elements of V-A group have five electrons in the valence band, each impurity atom will produce a free electron leaving the silicon negatively charged, the obtained material is named *n-type silicon*.

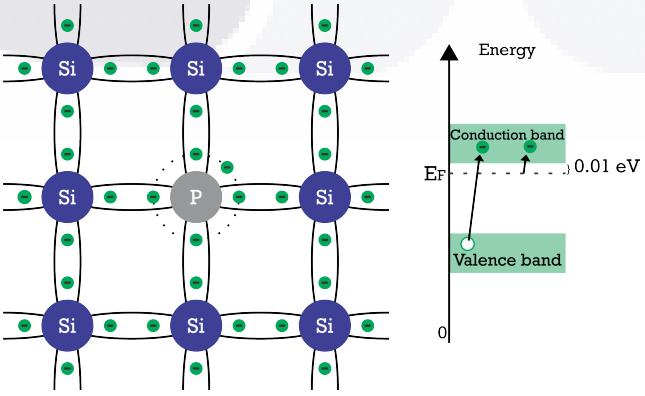

Figure 1.3: N-type semiconductor

On the other hand, when atoms of an element of the group III-A, as it is shown for boron in Figure 1.4, are added, a hole is produced for each impurity atom since the elements of III-A group has three electrons in the valence band, this way the silicon is positively charged, the obtained material is named *p-type silicon*.

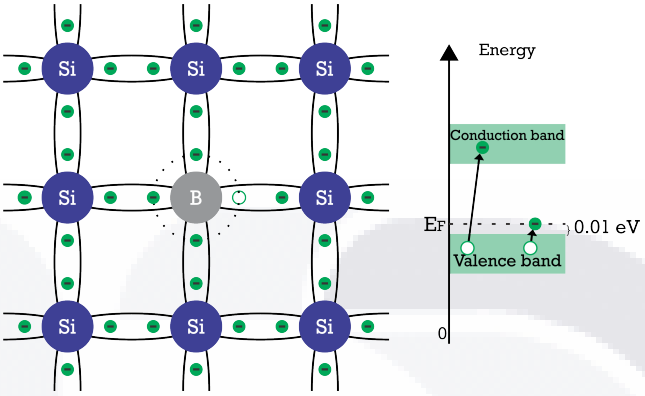

Figure 1.4: P-type semiconductor

1.1.2 P-N Junction

The region shared by an N-type and an P-type material when they are placed in touch is known as P-N junction. As we can see in Figure 1.5, there is a high concentration of electrons in the N-region and of the holes in the P-region, so they move according to their concentration gradient.

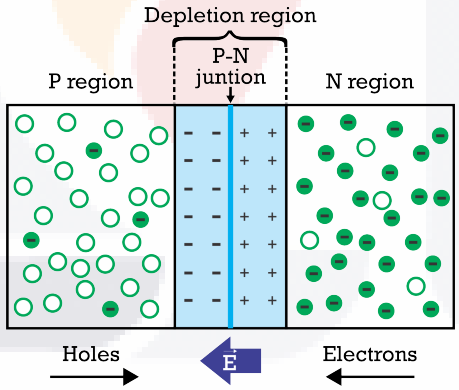

Figure 1.5: P-N Junction. The black arrows indicate how each type of carrier flows for one type semiconductor to the other.

When electrons from the N-region diffuse into the P-region, positively charged ions are left behind and the holes in the P-region which diffuse into N-region leave negatively charged ions near the P-N junction a neutrally charged region is created which is known as depletion region. On the other hand, the positive ions in the N-region and the negative ones in the P-region produce a "built-in" electric field that avoids the movement of charge carriers between the regions, this electric field is represented by the blue arrow in Figure 1.5. So, an external force will be required to move a charge carrier from one region to another such force is called barrier potential and is denoted by V_{bi}.

When a voltage is applied to the terminals of the junction, it is said to be biased, if the positive terminal of the voltage source is connected to the P side of the junction is said to be forward bias and if the positive terminal of the voltage source is connected to the N side of the junction is said to be reverse bias. The built-in voltage of a P-N junction is reduced or increased by the applied voltage V_a, this is given by

$$V_j = V_{bi} - V_a \tag{1.1.1}$$

where $V_a > 0$ for forward bias and $V_a < 0$ for reverse bias. When forward biased, the diffusion of electrons and holes in the junction is increased attempting to reestablish equilibrium, resulting in current flowing through the circuit. This will also affect the width of the depletion region as the value of V_{bi} change as we can see in Figure 1.6.

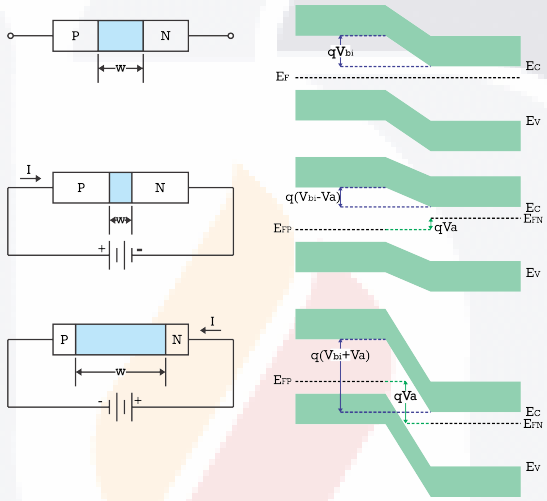

Figure 1.6: Effect of bias in a P-N junction, no bias (top), forward bias (middle), reverse bias (bottom)

1.1.3 Recombination of charge carriers

The generation of an electron-hole pair occurs when the electrons move from valence band to conduction band due to light absorption or increase of temperature. Meanwhile, recombination is the process where an electron-hole pair is annihilated [54].

The recombination processes can be divided in bulk and surface recombination [55], where bulk processes can also be subdivided in: radiative, Auger and Defect-assisted or SRH (for Shockley-Read-Hall). The first one consists in the transition of an electron from the conduction band into the valence band with a photon emission, the second one appears when an electron transfers its extra energy to another electron during a recombination process, the second electron will jump into a higher energy level and, when it relaxes, will release this extra energy as heat and the last one happens when the semiconductor contains trap states near the mid-gap. These recombination mechanisms are illustrated in Figure 1.7.

Meanwhile, surface recombination occurs when an interface between two different materials is created, i.e. at the front of a solar cell where the crystal lattice ends abruptly and a high concentration of defects is created, consequently when a minority carrier reaches a contact it can recombine with a

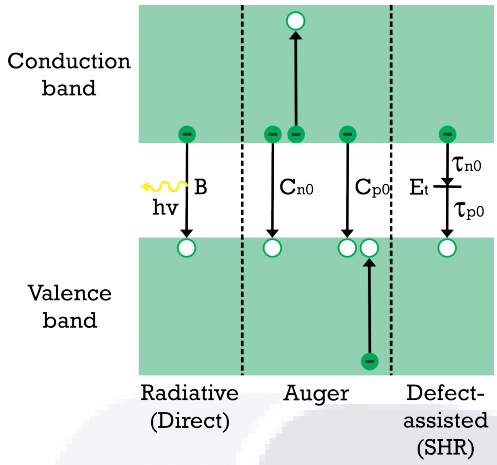

Figure 1.7: Bulk recombination mechanisms.

charge in the electrode [33].

1.2 Photovoltaic Effect

In this section we analyze the neccesary conditions for sunlight to generate a photocurrent in the solar cell, first we compare the energy emitted by the photons with the band gap in the solar cell (E_g) to determine whether or not this energy can generate electron-hole pairs. Afterthat, we present the mechanisms that occur inside and outside the depletion region so that electron-hole pairs contribute to the photocurrent.

As we can see in Figure 1.8 a certain amount of the sunlight is reflected and the rest can be absorbed or transmitted. The generation of an electron-hole pair due to the sunlight happens when the photon energy (E_{ph}) is greater or equal to the band gap (E_g) in the solar cell. However, it is important to point out that if $E_{ph} = E_g$ a transmission process can occur, that is, the photons will cross the solar cell without creating an electron-hole pair.

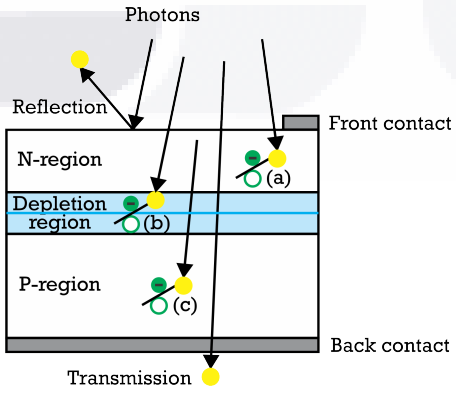

Figure 1.8: Possibilities for a photon (in yellow) in a solar cell. (a), (b) and (c) indicates electron-hole pair generation in the n-region, depletion region and p-region respectively.

The electron-hole pairs can be generated in any of the three regions of the solar cell: depletion region, P-region and N-region. If an electron-hole pair is generated inside the depletion region, by the action of the electric field, the electron is sent into the N-region and the hole to the P-region, producing thus a voltage between the terminals of the cell and/or a current flow into an external circuit. On the other hand, if an electron-hole pair is generated in the P-region the electron must travel a certain distance to arrive to the depletion region without recombining and be tossed into the N-region therefore it contributes to the photocurrent. In similar way, if an electron-hole pair is generated in the N-region, to contribute to the photocurrent, the hole must be able to travel a certain distance to reach the depletion region [56].

The distance traveled by a minority carrier γ, electron in the P-region and hole in the N-region, until the depletion region is called minority carrier diffusion length and is given by $L_\gamma = \sqrt{D_\gamma \tau_\gamma}$, where D_γ is the diffusion coefficient and τ_γ its lifetime [57]. The previous formula allows to determine the maximum width of each region in the solar cell since to avoid the recombination such width should be smaller that the corresponding diffusion length.

Summarizing, when a photon with enough energy creates an electron-hole pair that reaches the depletion region, see Figure 1.9, the action of the electric field will drift an electron towards the N-region (due to its positive charge) and a hole to the P-region (due to its negative charge). This way, electrons are collected by the contacts placed at the front of the cell and flow through an external circuit to the back contact in the P-region [52].

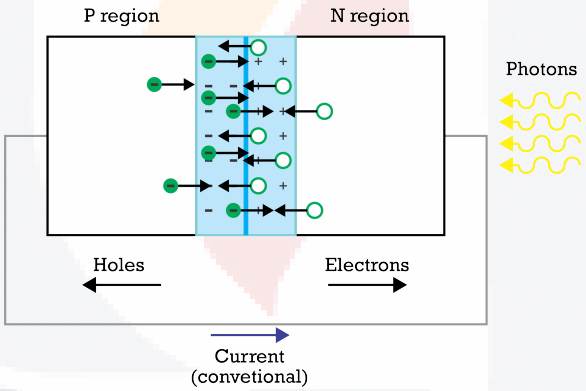

Figure 1.9: Photocurrent generation. The black arrows show how the carriers move when the equilibrium is broken by cause of radiation.

A solar cell has no external bias but when a photogenerated electron-hole pair is created, the minority carriers are swept down the energy barrier due to the build-in electric field as it can be appreciated in Figure 1.10. The photogenerated carriers create a new electric field E' with opposite direction than the build-in field meaning that the net electric field is given by $E - E'$, similar to a forward bias [58].

The creation of electron-hole pairs via the absorption of sunlight is essential to the operation of solar cells causing the transition of electrons from the valence band to the conduction bands, it is important to point out that during this process the energy and momentum of all the particles involved are conserved. The absorption coefficient varies according to the structure band of the semiconductor used for the manufacture of the solar cell. When the valence-band maximum occurs

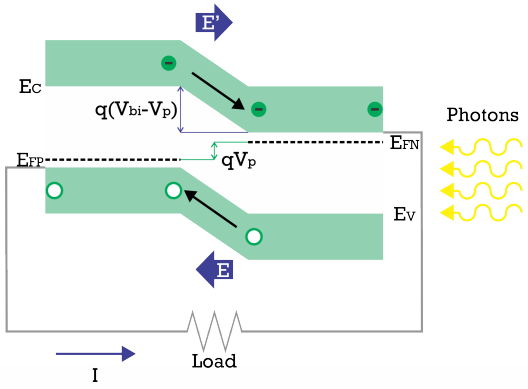

Figure 1.10: Band diagram of an illuminated solar cell.

at the same crystal momentum that the conduction-band minimum we say that the material posses a direct band structure and in the opposite case that posses a indirect band structure [54], see Figure 1.11.

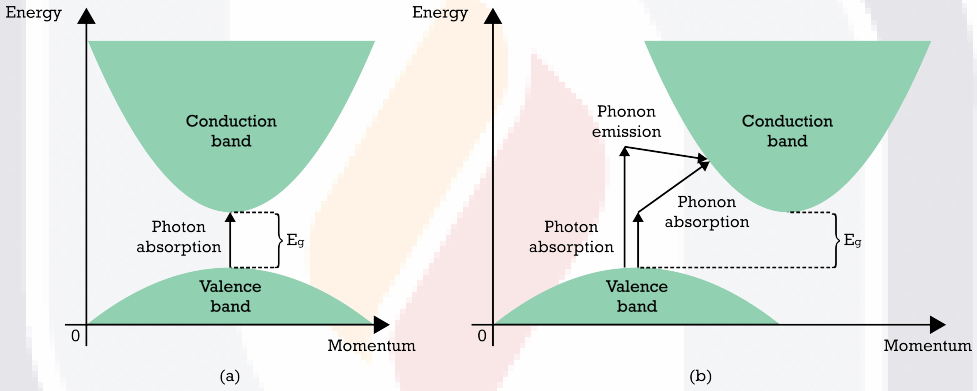

Figure 1.11: Direct (a) and indirect (b) band-gap.

In indirect band-gap semiconductors (as Si), their absorption coefficient are lower than those of direct band-gap semiconductors [54] since they require of photons and phonons (low energy particles with high momentum) to accomplish the transition of an electron from the valence band to the conduction band and to conserve the electron momentum. As a result of this, light penetrates more deeply in indirect band-gap semiconductor and to harness all it potentials is necessary to maximize the number of phonons with anti-reflective coatings and/or texturizing in order to maximize the effective thickness of the absorber [59].

2. Mathematical model

Most of the experimental works that aims to improve the efficiency of solar cells are focused in solar panels and the behavior of the efficiency when external phenomena as temperature [10, 64], absorption coat in the panel [8], rearrange of the contacts [11] and creation of new materials of the contacts [9] are modified. In this way, these surveys seek to improve the efficiency of a solar panel once the solar cell has already been manufactured.

Therefore, in this chapter we present a mathematical model that allows to study the change in the efficiency of a single solar cell through the modification of certain parameters involved in its manufacture. This model essentially describes the concentration of charge carriers (electrons and holes) in a single solar cell and considers phenomena such as diffusion, drift, recombination and generation.

2.1 Transport equations in semiconductors

The transport of charge carriers in a single semiconductor can be modeled by means of two macroscopic models: the hydrodynamic model and drift-diffusion model. The hydrodynamic model is obtained applying the entropy maximum principle to closure the moment equations of the Boltzmann equation and relates the interaction of electrons, holes and impurities (donors and acceptors) under the action of an electrical field, this model has been used to simulate a MOSFET device and a diode [19] and a GaAs solar cell [34]. On the other hand, the drift-diffusion model is determined by means of a scaling and posterior expansion of Boltzmann equations in which the collision operator is considered as the simple relaxation time approximation. Since drift-diffusion model has shown to reproduce in a good way the electronic behavior of a single semiconductor [33, 35, 67] and it is less complex than the hydrodynamic one, it will be used to model the photovoltaic effect in the solar cell.

2.1.1 Drift-diffusion equations

The drift-diffusion equations for a single semiconductor are given by

$$\begin{cases} \dfrac{\partial n}{\partial t} = \dfrac{1}{q}\nabla J_n + G - R \\ \dfrac{\partial p}{\partial t} = -\dfrac{1}{q}\nabla J_p + G - R \\ \operatorname{div}(\varepsilon \nabla \phi) = -q(p - n + N_D - N_A) \end{cases} \tag{2.1.1}$$

where n and p denote respectively the concentration of electrons and holes in the semiconductor, ϕ the electrostatic potential, q the electron charge and ε the permittivity. Also, G and R represent respectively the generation and recombination of charge carriers and, N_D and N_A are respectively the concentration of donor and acceptor impurities. Furthermore, the terms J_n and J_p defined as the net current density of electrons and holes , are given by

$$J_n = J_n(\text{diffusion}) + J_n(\text{drift}) = q\left(D_n \nabla n - \mu_n n \nabla \phi\right), \tag{2.1.2}$$

$$J_p = J_p(\text{diffusion}) + J_p(\text{drift}) = -q\left(D_p \nabla p + \mu_p p \nabla \phi\right), \tag{2.1.3}$$

with D_n and D_p the respective diffusion coefficients of electrons and holes and, μ_n and μ_p are their respective mobility coefficients.

2.2 Mathematical modeling of the solar cell

In this section we use the drift-diffusion equations (2.1.1)-(2.1.3) to model the photovoltaic effect in a solar cell. We first mathematically characterize the three electronic regions in a solar cell, after, analyze the contributions of the generation and the recombination of charge carriers and show the variation of the electrostatic potential throughout the cell and, finally tacking into account the suitable initial and boundary conditions we present the mathematical model obtained.

2.2.1 Spatial domain

Let x_p, d_p, d_n and x_n be positive real numbers with $d_p < x_p$ and $d_n < x_n$ and let also be $\Omega = (-x_p, x_n)$ a open set of $\mathbb{R}$ such that $\overline{\Omega}$ is the union of the subsets $\Omega_p^* = \left(-x_p, -d_p\right)$, $\Omega_d = \left(-d_p, d_n\right)$ and $\Omega_n^* = (d_n, x_n)$ and their corresponding boundaries denoted by $\partial\Omega_p^* = \left\{-x_p, -d_p\right\}$, $\partial\Omega_d = \left\{-d_p, d_n\right\}$ and $\partial\Omega_n^* = \{d_n, x_n\}$.

Therefore, as we can see in Figure 2.1, the three electronic regions: the P-region that does not belong to the depletion region, the depletion region and the N-region that is not in the depletion region are respectively represented by: Ω_p^*, Ω_d and Ω_n^*.

2.2.2 Generation of charge carriers

The mechanism of generation of charge carriers by means of light was introduced by Gärtner in 1959 [65], he considered a photon flux F produced by a monochromatic light of intensity I_f on the cell's surface with $F = \dfrac{\lambda I_f}{hc}$, where λ and c are respectively the wavelength and the speed of light, and h

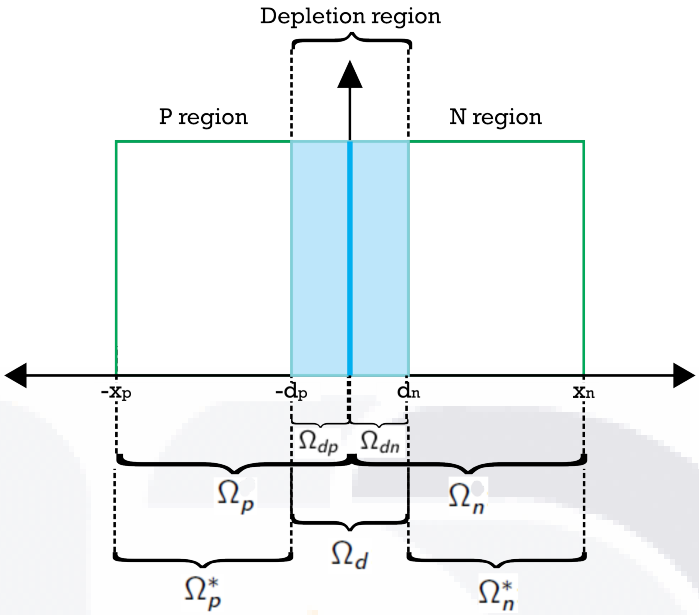

Figure 2.1: In a solar cell the regions: Ω_p^*, Ω_d and Ω_n^* are electronically formed between the physical regions Ω_p and Ω_n.

is the Planck's constant. Taking into account that a part of the light is reflected, the term $(1-r)F$ represents the absorbed photon flux, where r is the reflection coefficient of the cell. From Lambert's law (also known as Bouguer's law) we know that the absorbed photon flux decays exponentially with the distance into the material, this way, the net absorbed photon flux $\tilde{F}$ is given by

$$\tilde{F} = (1-r)Fe^{-\alpha x}$$

with α as the absorption coefficient of the light with a wavelength λ. On the other hand, under the assumption that an electron-hole pair is created for each absorbed photon, the rate of generation is given by

$$G = \lim_{\Delta x \to 0} \frac{\tilde{F}(x) - \tilde{F}(x+\Delta x)}{\Delta x} = -\frac{d}{dx}\tilde{F}(x) = \alpha \hat{F} e^{-\alpha x} \tag{2.2.1}$$

where $\hat{F} = \dfrac{(1-r)\lambda}{hc} I_f$.

2.2.3 Recombination of charge carriers

There are three types of recombination of charge carriers: radiative (R_λ), Auger (R_{Auger}) and Defect-assisted (R_{SRH}), see Section 1.1.3. This way, by considering the contribution of each type of recombination R is given by

$$R = \left[\sum_{trapsj} R_{SRHj}\right] + R_\lambda + R_{Auger}, \tag{2.2.2}$$

where

$$R_{SRHj} = \frac{pn - n_i^2}{\tau_{SRH,n}\left(p + p_j\right) + \tau_{SRH,p}\left(n + n_j\right)}, \tag{2.2.3}$$

$$R_{\lambda} = B_{\lambda}(pn - n_i^2), \tag{2.2.4}$$

$$R_{Auger} = (C_n n + C_p p)(pn - n_i^2). \tag{2.2.5}$$

Here, n_i is the intrinsic carrier concentration, B_λ the radiative recombination coefficient [40] and, C_n and C_p are respectively the Auger recombination coefficients for electrons and holes [41]. Meanwhile, $\tau_{SRH,n}$ and $\tau_{SRH,p}$ represent the lifetime of electrons and holes in SRH recombination [106], respectively.

The recombination rate is governed by the minority carrier density, consequently, let $\overline{\omega}$ and $\underline{\omega}$ be, respectively, the majority and minority carrier density whose initial densities are given by $\overline{\omega}_0$ and $\underline{\omega}_0$. Assuming that $\underline{\omega}_0 \leq \underline{\omega} \ll \overline{\omega}_0$ it gets

$$\begin{aligned} R_{SRH,\underline{\omega}} &\approx \frac{\underline{\omega} - \underline{\omega}_0}{\tau_{SRH,\underline{\omega}}}, \\ R_{\lambda,\underline{\omega}} &\approx \frac{\underline{\omega} - \underline{\omega}_0}{\tau_{\lambda,\underline{\omega}}}, \\ R_{Auger,\underline{\omega}} &\approx \frac{\underline{\omega} - \underline{\omega}_0}{\tau_{Auger,\underline{\omega}}}. \end{aligned}$$

Therefore, the recombination rate for the minority and majority carriers is given by

$$\begin{aligned} R_{\underline{\omega}} = &\quad R_{SRH,\underline{\omega}} + R_{\lambda,\underline{\omega}} + R_{Auger,\underline{\omega}} \approx \tfrac{\underline{\omega} - \underline{\omega}_0}{\tau_{\underline{\omega}}} \\ R_{\overline{\omega}} = 0 & \end{aligned}$$

where $\tau_{\underline{\omega}} = \dfrac{1}{\tau_{SRH,\underline{\omega}}} + \dfrac{1}{\tau^R_{\lambda,\underline{\omega}}} + \dfrac{1}{\tau_{Auger,\underline{\omega}}}$ is the minority carrier lifetime.

Since the electrons (n) are minority carriers in Ω_p^* and the holes (p) in Ω_n^* and, there are not free carriers in the depletion region Ω_d. The recombination rate for the three electronic regions are shown in Table 2.1.

Region/Rate	R_n	R_p
Ω_p^*	$\dfrac{n - n_0}{\tau_n^R}$	0
Ω_d	0	0
Ω_n^*	0	$\dfrac{p - p_0}{\tau_p^R}$

Table 2.1: Recombination in each electronic region.

2.2.4 Electrostatic potential

The electrostatic potential and the density of charge carriers and impurities, in a semiconductor, are related by means of the Poisson equation $\mathrm{div}(\varepsilon \nabla \phi) = -q\rho$ where ρ is the net charge in a specific electronic region. According to the electronic behavior of the P-N junction, which was presented in

Section 1.1.2, we have that

$$\operatorname{div}(\varepsilon\nabla\phi) = \begin{cases} -q(p-n-N_A) & \text{in} \quad \Omega_p^* \\ -q(N_D-N_A) & \text{in} \quad \Omega_d \\ -q(p-n+N_D) & \text{in} \quad \Omega_n^* \end{cases} \tag{2.2.6}$$

2.2.5 Initial, boundary and jump conditions

Initial conditions

Given that at the beginning there is no recombination and generation of charge carriers and considering that the solar cell is in equilibrium, that is, there is no current due to drift or diffusion of carriers, the initial conditions for electrons and holes are given by

$$n(x,t) = \begin{cases} 0 & \text{in} \quad \Omega_p^* \times \{t=0\} \\ 0 & \text{in} \quad \Omega_d \times \{t=0\} \\ N_D(x) & \text{in} \quad \Omega_n^* \times \{t=0\} \end{cases} \tag{2.2.7}$$

$$p(x,t) = \begin{cases} N_A(x) & \text{in} \quad \Omega_p^* \times \{t=0\} \\ 0 & \text{in} \quad \Omega_d \times \{t=0\} \\ 0 & \text{in} \quad \Omega_n^* \times \{t=0\} \end{cases} \tag{2.2.8}$$

The initial value for electric potential ϕ is determined solving the Poisson equation (2.2.6) when n and p are respectively given by (2.2.7) and (2.2.8).

Remark 2.1. It is often assumed that the carrier densities obey the Maxwell-Boltzmann statistics and that N_D, N_A and ε are constant, under such assumptions the initial value for ϕ is

$$\phi(x) = \begin{cases} \phi_p & \text{in} \quad \Omega_p^* \times \{t=0\} \\ q\dfrac{N_A}{2\varepsilon}\left(x+d_p\right)^2 & \text{in} \quad \Omega_{dp} \times \{t=0\} \\ q\dfrac{N_D}{\varepsilon}\left(d_n - \dfrac{x}{2}\right)x + q\dfrac{N_A}{2\varepsilon}d_p^2 & \text{in} \quad \Omega_{dn} \times \{t=0\} \\ \phi_n & \text{in} \quad \Omega_n^* \times \{t=0\} \end{cases} \tag{2.2.9}$$

Boundary conditions

To close the circuit in the solar cell two metals are placed at $x = -x_p$ and $x = x_n$, these types of contacts metal-semiconductor are modeled by imposing of Dirichlet boundary conditions

$$n(x,t) = n_{eq}(x), \tag{2.2.10}$$

$$p(x,t) = p_{eq}(x), \tag{2.2.11}$$

$$\phi(x,t) = V_{bi} + \phi_{ph}, \tag{2.2.12}$$

where $\phi_{ph} = \phi_{ph}^n + \phi_{ph}^p$ is the photogenerated potential which is the sum of the potentials generated at the edges of the cell. Additionally, we establish that $\phi(0) = 0$ and, to maintain the charge neutrality

at equilibrium in Ω_p^* and Ω_n^*

$$\nabla E = \operatorname{div}(\varepsilon \nabla \phi) = 0.$$

The conditions (2.2.10)-(2.2.12) are determined in a equilibrium solar cell for which the current densities are zero, that is

$$\begin{cases} D_n \nabla n - \mu_n n \nabla \phi &= 0, \\ D_p \nabla p + \mu_p p \nabla \phi &= 0, \end{cases}, \tag{2.2.13}$$

also the neutrality charge and the law of mass action

$$\begin{cases} N_D(x) - N_A(x) + p_{eq}(x) - n_{eq}(x) &= 0, \\ n_{eq}(x)\, p_{eq}(x) &= n_i^2, \end{cases} \tag{2.2.14}$$

are kept. From (2.2.14) it follows that

$$n_{eq}(x) = \frac{1}{2}\left(\sqrt{(N_D(x) - N_A(x))^2 + 4n_i^2} + N_D(x) - N_A(x)\right) \tag{2.2.15}$$

and

$$p_{eq}(x) = \frac{1}{2}\left(\sqrt{(N_D(x) - N_A(x))^2 + 4n_i^2} - N_D(x) + N_A(x)\right). \tag{2.2.16}$$

Given that outside of depletion region electric field is negligible we assume that the electric potential is constant there. Therefore, if F_1 and F_2 are functions defined by $\phi(x) = F_1(x, n(x)) = F_2(x, p(x))$ such that are solutions of system (2.2.13) then V_{bi} defined as $V_{bi} = \phi(d_n) - \phi(-d_p)$ is given by

$$V_{bi} = F_1\left(d_n, n_{eq}(d_n)\right) - F_1\left(-d_p, n_{eq}(-d_p)\right) = F_2\left(d_n, p_{eq}(d_n)\right) - F_2\left(-d_p, p_{eq}(-d_p)\right). \tag{2.2.17}$$

Remark 2.2. Note that we have only assumed that the electric field is constant outside of depletion region. For which the boundary conditions obtained by the systems (2.2.13) and (2.2.14) are much general than the existing works. These conditions are commonly determined considering the solar cell as an ideal diode as can be seen in Appendix A .

Jump conditions

A very complicated issue in the modeling of the solar cell is to impose suitable boundary conditions, if we think from the mathematical point of view then we want to obtain a sufficiently smooth solution along the domain but such boundary conditions are not consistent with the physical part. On the other hand, some boundary conditions are only valid if the process satisfies certain assumptions which are not applicable with the particular phenomenon [67, 101].

For lightly doped semiconductors where the P-N junction is homogeneous, a Schottky contact is considered for which the electrostatic potential at the interfaces $x = -d_p$ and $x = d_n$ is given by [41]

$$[\phi]_{-d_p} = \phi_{-d_p^-} - \phi_{-d_p^+} = 0, \qquad \left[\frac{\partial \phi}{\partial x}\right]_{-d_p} = \left.\frac{\partial \phi}{\partial x}\right|_{-d_p^-} - \left.\frac{\partial \phi}{\partial x}\right|_{-d_p^+} = 0 \tag{2.2.18}$$

$$[\phi]_{d_n} = \phi_{d_n^-} - \phi_{d_n^+} = 0, \qquad \left[\frac{\partial \phi}{\partial x}\right]_{d_n} = \left.\frac{\partial \phi}{\partial x}\right|_{d_n^-} - \left.\frac{\partial \phi}{\partial x}\right|_{d_n^+} = 0. \tag{2.2.19}$$

Meanwhile, the current densities satisfy the following conditions [68, 66]

$$[J_n \cdot \nu]_{-d_p} = J_n \cdot \nu|_{-d_p^-} - J_n \cdot \nu|_{-d_p^+} = -v_{n,-d_p}\left(n - n_{eq}\right), \qquad [J_n \cdot \nu]_{d_n} = J_n \cdot \nu|_{d_n^-} - J_n \cdot \nu|_{d_n^+} = -v_{n,d_n}\left(n - n_{eq}\right)$$
$$\left[J_p \cdot \nu\right]_{-d_p} = J_p \cdot \nu\Big|_{-d_p^-} - J_p \cdot \nu\Big|_{-d_p^+} = v_{p,-d_p}\left(p - p_{eq}\right), \qquad \left[J_p \cdot \nu\right]_{d_n} = J_p \cdot \nu\Big|_{d_n^-} - J_p \cdot \nu\Big|_{d_n^+} = v_{p,d_n}\left(p - p_{eq}\right)$$

where $v_{\gamma,x}$ represents the recombination velocity of carrier γ ($\gamma = \{\text{electron}, \text{hole}\}$) at point x and the superscripts $-$ and $+$ indicates respectively the left and right side of the interface.

In the case of heavily doped semiconductors, the above conditions are not applicable. In this sense, the problem of finding suitable interface conditions for semiconductors that does not satisfy the assumptions of a ideal p-n junction, see Appendix A, is still a open problem [66, 67].

Remark 2.3. To increase the efficiency of a solar cell, we must first analyze different situations such as doping at different levels, doping profile, diffusion coefficients dependent on the electric field among others, before imposing boundary and interface conditions that are physically consistent.

2.3 Mathematical model

The following set of systems of differential equations under the boundary and interface conditions analyzed in Subsection 2.2.5 constitutes our mathematical model for a solar cell that, as we will see in the next section, allows us to study the efficiency of solar cell by means of the variables n, p and ϕ of the model.

$$\begin{cases} \dfrac{\partial n}{\partial t} = \dfrac{1}{q}\dfrac{\partial}{\partial x}J_n + \alpha \hat{F} e^{-\alpha x} - \dfrac{n - n_0}{\tau_n^R} & \text{in } \Omega_p^* \times (0,T] \\ \dfrac{\partial p}{\partial t} = -\dfrac{1}{q}\dfrac{\partial}{\partial x}J_p + \alpha \hat{F} e^{-\alpha x} & \text{in } \Omega_p^* \times (0,T] \\ \dfrac{\partial}{\partial x}\left(\varepsilon \dfrac{\partial \phi}{\partial x}\right) = -q(p - n - N_A) & \text{in } \Omega_p^* \times (0,T] \\ n(x,t) = n_{eq}(x), \quad p(x,t) = p_{eq}(x), \quad \phi(x) = V_{bi} + \phi_{ph}^p & \text{on } \left\{x = -x_p\right\} \times (0,T] \\ n(x,t) = 0, \quad p(x,t) = N_A, \quad \dfrac{\partial}{\partial x}E = -\dfrac{\partial}{\partial x}\left(\varepsilon \dfrac{\partial \phi}{\partial x}\right) = 0 & \text{on } \Omega_p^* \times \{t = 0\} \end{cases} \tag{2.3.1}$$

$$\begin{cases} \dfrac{\partial n}{\partial t} = \dfrac{1}{q}\dfrac{\partial}{\partial x}J_n + \alpha \hat{F} e^{-\alpha x} & \text{in } \Omega_d \times (0,T] \\ \dfrac{\partial p}{\partial t} = -\dfrac{1}{q}\dfrac{\partial}{\partial x}J_p + \alpha \hat{F} e^{-\alpha x} & \text{in } \Omega_d \times (0,T] \\ \dfrac{\partial}{\partial x}\left(\varepsilon \dfrac{\partial \phi}{\partial x}\right) = -q(N_D - N_A) & \text{in } \Omega_d \times (0,T] \\ n(x,t) = 0, \quad p(x,t) = 0 & \text{on } \Omega_d \times \{t = 0\} \\ \phi(x) = 0 & \text{on } \{x = 0\} \times \{t = 0\} \end{cases} \tag{2.3.2}$$

$$\begin{cases} \dfrac{\partial n}{\partial t} = \dfrac{1}{q}\dfrac{\partial}{\partial x}J_n + \alpha \hat{F} e^{-\alpha x} & \text{in } \Omega_n^* \times (0,T] \\ \dfrac{\partial p}{\partial t} = -\dfrac{1}{q}\dfrac{\partial}{\partial x}J_p + \alpha \hat{F} e^{-\alpha x} - \dfrac{p-p_0}{\tau_p^R} & \text{in } \Omega_n^* \times (0,T] \\ \dfrac{\partial}{\partial x}\left(\varepsilon \dfrac{\partial \phi}{\partial x}\right) = -q(p-n+N_D) & \text{in } \Omega_n^* \times (0,T] \\ n(x,t) = n_{eq}(x), \quad p(x,t) = p_{eq}(x), \quad \phi(x_n) = V_{bi} + \phi_{ph}^n & \text{on } \{x = x_n\} \times (0,T] \\ n(x,t) = N_D, \quad p(x,t) = 0, \quad \dfrac{\partial E}{\partial x} = -\dfrac{\partial}{\partial x}\left(\varepsilon \dfrac{\partial \phi}{\partial x}\right) = 0 & \text{on } \Omega_n^* \times \{t = 0\} \end{cases} \tag{2.3.3}$$

Remark 2.4. The model (2.3.1)-(2.3.3) is also applicable for heavily doped semiconductors applying the generalized Einstein relations (A.2.1) in the current densities J_n and J_p given in (2.1.2) and (2.1.3), respectively.

Remark 2.5. The interval $(0,T]$ represents the temporal domain.

2.3.1 Solar cell eficiency

The main objective of this work is to improve the efficiency of a solar cell for wich we will show as the variables of the model (2.3.1)-(2.3.3) allow to address it.

The efficiency (η) in the solar cell is the relation between the generated power and the incident power (P_i) given by

$$\eta = \frac{I_{\max} V_{\max}}{P_i} \tag{2.3.4}$$

where $I_{\max}$ and $V_{\max}$ are respectively the maximum current and voltage in the cell. Firstly, since the total current is related with the current density J by

$$I(t) = \int_\Omega J \cdot dS,$$

and

$$J(n,p,\phi) = J_n + J_p = q\left(D_n \nabla n - \mu_n n \nabla \phi\right) - q\left(D_p \nabla p + \mu_p p \nabla \phi\right),$$

then, the total current in the cell is given by

$$I(t) = q \int_\Omega \left[\left(D_n \nabla n^* - D_p \nabla p^*\right) - \left(\mu_n n^* + \mu_p p^*\right)\nabla \phi^*\right] \cdot dS \tag{2.3.5}$$

here, $(n(x,t), p(x,t), \phi(x)) = (n^*(x,t), p^*(x,t), \phi^*(x))$ represents the solution of model (2.3.1)-(2.3.3). On the other hand, the voltage in the cell is defined as the potential difference between the terminals $x = -x_d$ and $x = x_n$, therefore

$$V\Big|_{x=-x_d}^{x=x_n} = \phi^*(x_n) - \phi^*(-x_d) \tag{2.3.6}$$

Remark 2.6. The formulas (2.3.5) and (2.3.6) for the current and voltage in the cell are obtained considering lightly doped semiconductors, for heavily doped semiconductors or a combination of both it is necessary a complete analysis to obtain the corresponding formulas.

3. Qualitative analysis

In this chapter, we determine according to the existing mathematical models the most relevant parameters that might allow us to improve the efficiency in the model (2.3.1)-(2.3.3). We also present the mathematical results about of important aspects over the mathematical model.

3.1 Important Parameters

Here, we present the parameters that allow in the model (2.3.1)-(2.3.3) improve the efficiency in a solar cell. Moreover, we show the assumptions carried out in similar mathematical models existing in the literature.

1. **Mobility coefficients**

   (i) *Constant:* reference values for μ_n and μ_p respectively are 1400 $\mathrm{cm}^2/(\mathrm{V}\cdot\mathrm{s})$ and 470 $\mathrm{cm}^2/\mathrm{V}\cdot\mathrm{s}$ [70].

   (ii) *Function of the temperature:* If the doping levels are low the mobility is governed by intrinsic lattice scattering, $\mu_L = C_L T^{-3/2}$ where T is the temperature and C_L is a constant [54], meanwhile, if the doping is high the ionized impurity scattering controls the scattering, $\mu_I = \dfrac{C_I T^{3/2}}{N_D + N_A}$ with C_I a constant [54]. On the other hand. when more than one scattering type is considered, the mobility coefficient is obtained as the reciprocal of the sum of each scattering mechanism contribution reciprocal.

   (iii) *Function of impurity concentrations* The mobility coefficients can be estimated by the following empirical formulas [54, 70]

$$\mu_n = 92 + \frac{1318}{1 + \left[(N_A + N_D)/1\times 10^{17}\right]^{0.85}} \quad [cm^2/(\mathrm{V}\cdot\mathrm{s})]$$

   and

$$\mu_p = 50 + \frac{420}{1 + \left[(N_A + N_D)/1.6\times 10^{17}\right]^{0.7}} \quad [cm^2/(\mathrm{V}\cdot\mathrm{s})].$$

(iv) *Function of the electric potential:*

$$\mu_n = \mu_n^0\left(1+\frac{\mu_n^0|\nabla\phi|}{v_n}\right)^{-1} \qquad \text{and,} \qquad \mu_p = \mu_p^0\left(1+\frac{\mu_p^0|\nabla\phi|}{v_p}\right)^{-1}$$

where μ_n^0 and μ_p^0 are respectively field-independent scattering mobility coefficients of electrons and holes [44].

2. **Diffusion coefficients**

(i) *Constant:* common values for D_n and D_p are respectively $20\text{cm}^2/\text{s}$ and $3\text{cm}^2/\text{s}$ [37].

(ii) *Function of the electric potential:* under the assumptions that the Einstein relations are fulfilled and that the diffusion coefficients are functions of the mobility coefficients, which are dependent on the electric potential, it follows that [44]

$$D_\gamma = \mu_\gamma(-\nabla\phi) + \frac{2}{3}\tau_\gamma\left[\mu_\gamma(-\nabla\phi)|-\nabla\phi|\right]^2, \qquad \gamma = n, p.$$

3. **Absorption coefficient**

(i) *Constant:* its value is normally determined for a specific wavelength or obtained as an average of a selected range of wavelengths, i.e. $9.52\times10^4\ \text{cm}^{-1}$ for 400 nm [74].

(ii) *Function of the extinction coefficient:* Beer-Lambert' s law relates the absorption coefficient (α), the extinction coefficient (κ_e) and incident wavelength (λ) by means of the formula $\alpha = \frac{4\pi\kappa_e}{\lambda}$ [56].

(iii) *Function of the temperature:*

$$\alpha = \sum_{i,j=1,2} C_i A_j \left\{\frac{[\hbar\nu - E_{gi}(T) + E_{pi}]^2}{e^{E_{pi}/KT-1}} + \frac{[\hbar\nu - E_{gi}(T) - E_{pi}]^2}{1-e^{-E_{pi}/KT}}\right\} + A_d[\hbar\nu - E_{gd}(T)]^{1/2},$$

for $20\text{K} \le T \le 500\text{K}$, the values of functions and constants are given in [75].

4. **Doping profile**

(i) *Constant:* some reference values for N_D and N_A, respectively, are $1\times10^{20}\text{cm}^{-3}$ and $1\times10^{15}\text{cm}^{-3}$ [54], $1\times10^{19}\text{cm}^{-3}$ and $1.5\times10^{16}\text{cm}^{-3}$ [37], $5\times10^{14}\text{cm}^{-3}$ and $1\times10^{13}\text{cm}^{-3}$ [56]

(ii) *Function of space:* some doping profiles are the following

$$\begin{cases} \text{Gaussian} & \Rightarrow \quad N_{A(D)}(x) = N_0 e^{-x^2/(4D_\gamma t)} \\ \text{Complementary error} & \Rightarrow \quad N_{A(D)}(x) = N_0\text{erfc}\left(\dfrac{x}{2\sqrt{D_\gamma t}}\right) \\ \text{Rxponential} & \Rightarrow \quad N_{A(D)}(x) = N_0 e^{x/(2\sqrt{D_\gamma t})} \end{cases}$$

where t is a period of time, N_0 is the doping concentration at the surface and γ is either n for N_D or p for N_A [35].

5. **Cell width**

   To avoid the recombination of charge carriers, the width of regions n and p should be limited by the diffusion length

   $$L_\gamma = \sqrt{D_\gamma \tau_\gamma}, \quad \gamma = n, p.$$

   Some reference values for x_n and x_p are respectively 0.35μm and 300μm [54], and 0.2nm and 300nm [56].

6. **Permittivity**

   (i) *Constant*: an usual value is 1.04×10^{-12}F/cm or its relative value respect the vacuum permittivity (8.854×10^{-12}F/m) is 11.7.

   (ii) *Function of temperature:* the value of the permittivity increases as the temperature increases due to the activation of different polarization mechanisms.

   (iii) *Function of space:* if the solar cell is composed by different materials the permittivity will vary between regions, this way, sometimes it is considered as a piecewise constant function [67].

7. **Generation term**

   (i) *Function of absorption coefficient:*

   $$G = \alpha \hat{F} e^{-\alpha x}$$

   where α is the absorption coefficient and $\hat{F}$ the absorbed photon flux [65].

   (ii) *Function of direction:*

   $$G = \begin{cases} \alpha(x) G_0(x_0) e^{\int_0^s \alpha(x_0 + s'\theta_0) ds'} & \text{if } x = x_0 + x\theta_0 \\ 0 & \text{otherwise,} \end{cases}$$

   where the absorption coefficient $\alpha(x)$ is integrated over the usable spectrum, x_0, θ_0 and G_0 are the incident location, direction and photon flux [41].

   (iii) *Interaction between generation and recombination:* A particular form for the recombination and generation terms is the one presented by Carlo de Falco et al. [72] where they are governed by the additional differential equation

   $$\begin{cases} \dot{X} &= g - r \\ g &= \underbrace{G(x,t)}_{(a)} + \underbrace{\zeta p n}_{(b)} \\ r &= \underbrace{k_{diss} X}_{(c)} + \underbrace{k_{rec} X}_{(d)} \end{cases}$$

   where (a) provides the photo-generation rate, (b) the recombination rate, (c) the separation rate of a bound pair and (d) the recombination rate of electron-hole pairs that are not split.

8. **Recombination term**

   (i) *Shockley-Read-Hall Recombination:*

$$R_{SRH} = \frac{pn - n_i^2}{\tau_{SRH,n}(p + n_i) + \tau_{SRH,p}(n + n_i)},$$

   where n_i is the intrinsic carrier concentration, meanwhile, $\tau_{SRH,n}$ and $\tau_{SRH,p}$ represent respectively the lifetime of electrons and holes [106].

   (ii) *Auger recombination:*

$$R_{Auger} = (C_n n + C_p p)(pn - n_i^2),$$

   C_n and C_p are respectively the Auger recombination coefficients for electrons and holes [41].

   (iii) *Radiative recombination:*

$$R_\lambda = B_\lambda(pn - n_i^2),$$

   here, B_λ is the radiative recombination coefficient [40].

3.2 Existing drift-difusion models

Here, we enlist some models based on the drifft-diffusion equations which have been used to describe the concentration of charge carriers and the electric field in a single semiconductor. Although the model (2.3.1)-(2.3.3) is more complex, due to the coupling in the interfaces, these works allow to observe whether or not its solution will possess the following properties:

1. **Existence of solutions**

   (i) Under the assumption that $D_n = \mu_n$ and $D_p = \mu_p$ and positive bounded mobility coefficients of the form $\mu = \left(x, \left|\nabla\phi\right|\right)$ Beirao da Veiga [78], shows by the Schauder fixed theorem and the upper and lower solutions that the drift-diffusion model has a weak steady state solution.

   (ii) Unlike da Veiga, Frehse and Naumann [79] prove the existence of a positive weak steady state solution, if the diffusion coefficients and the saturation velocity are bounded, that is, there exist K_i and M_i positive such that $0 < D_i < K_i$ and $\mu_i \left|\nabla\phi\right| < M_i$.

   (iii) Falco et al. [72] presents a weak solution existence theorem for the stationary state by assuming that ζ, k_{diss}, k_{rec} and $G(x,t)$ are positive constants, the Einstein relations are satisfied, the voltage is bounded, $\kappa_\gamma = 0$ and β_γ, α_γ are position functions only, additionally, in the case of transient regime, also a theorem is proposed establishing that the model admits a weak solution (ϕ, u), where $u := (n, p)$, such that:

      (a) $u > 0$ a.e. Ω_T

      (b) $u(x,0) = U(x,0)$ and $u - U \in L^2(0,T;H_o)^2$

      (c) $u \in (C(0,T;L^2(\Omega)) \cap L^\infty(\Omega_T))^2$

      (d) $\dfrac{\partial u}{\partial t} \in L^2(0,T;H_0')^2$

(e) $\phi - \Psi \in L^2(0,T;H_0)$ with $\phi \in L^\infty(\Omega_T)$

where $U := (n_0, p_0) \in (H^1(\Omega_T) \cap L^\infty(\Omega_T))^2$ and $\Psi \in H^1(\Omega_T) \cap L^\infty(\Omega_T)$ is a function representing a lifting of the electric potential boundary conditions.

2. **Global solutions**

   (i) Fang e Ito [80] proves the existence of a global weak solution when the mobility of charge carriers is a bounded lipschitz and the recombination term is locally lipschitz continuous.

   (ii) Nagai and Ogawa [81] show that the drift-diffusion model without the recombination and generation terms has a non-negative global solution for the Cauchy problem whenever the initial data u_0 satisfies that $u_0(1+|x|) \in L^1(\mathbb{R}^2)$.

3. **Boundedness of solutions**

   (i) Beirao da Veiga in [78] also proves that as the time-dependent solution as the steady state solution of the drift-diffusion equations is uniformly bounded if the diffusion and mobility of charge carriers are constant.

   (ii) Flores and Jerez assumming that the Nernst-Einstein relation is satisfied and considering the current density constant proved by means of the upper and lower solutions technique the boundedness of the solution if a homogeneous Neumann boundary condition is imposed.

4. **Asymptotic behavior**

   (i) For the drift-diffusion equations with zero Neumann conditions and $D_n = D_p = \mu_n = \mu_p = 1$, Mock shows that the time dependent solution decays exponentially to its unique steady state solution whenever the impurity profile in the semiconductor let be constant [83]. Moreover, he proves that the electrical potential ϕ is bounded in the norm L_1 where the constant depends on the initial data and the impurity profile.

   (ii) Assuming the diffusion and mobility of charge carriers constant, a differentiable and bounded recombination term as well as the impurity profile and the generation term are in $L^\infty(\Omega)$, Fang and Ito [80] proves the existence of a compact, connected and maximal attractor.

3.3 Mathematical and numerical analysis

In this section we analyze the mathematical and numerical aspects in the model (2.3.1)-(2.3.3) such as: the existence and uniqueness of the solution, the need to obtain a numerical method that conserves the electron and hole densities as well as their positivity, the analysis of the singularly perturbed system obtained by means of a suitable scalling and finally the study of numerical methods used to tackle the coupling in the interfaces.

3.3.1 Existence and Uniqueness

In the case of steady state the variables n and p are commonly changed in terms of quasi-Fermi levels ϕ_n and ϕ_p by means of the Maxwell-Boltzmann statistic

$$n = n_i e^{\frac{q(\phi-\phi_n)}{kT}}, \qquad p = n_i e^{\frac{q(\phi_p-\phi)}{kT}}, \tag{3.3.1}$$

it is important to note that this relation is valid only for low carrier densities, however, if the semiconductor has a high density of carriers then the above relation should be substituted by the Fermi-Dirac statistic [87]. On the other hand, when the Einstein relation is held some works use the Slotboom formulation [76, 77]

$$n = n_i e^{\frac{\phi}{U_T}}\Phi_n, \qquad p = n_i e^{\frac{-\phi}{U_T}}\Phi_p, \tag{3.3.2}$$

where U_T is the thermal voltage. Although under anyone of these formulations the positivity of their respective variables is ensured, in terms of the variables (ϕ, ϕ_n, ϕ_p) the differential operators of the continuity equations are nonlinear meanwhile in terms of the variables $\left(\phi, \Phi_n, \Phi_p\right)$ the differential operators are linear and self-adjoint [88]. This way, by means of the relation (3.3.2) the drift-diffusion model can be rewritten as follows

$$\begin{aligned}
\varepsilon\Delta\phi &= qn_i\left(\Phi_n e^{\frac{\phi}{U_T}} - \Phi_p e^{\frac{-\phi}{U_T}}\right) - qC(x),\\
n_i U_T \nabla\cdot(\mu_n e^{\frac{\phi}{U_T}}\nabla\Phi_n) &= R\left(\phi, \Phi_n, \Phi_p\right),\\
n_i U_T \nabla\cdot(\mu_p e^{\frac{-\phi}{U_T}}\nabla\Phi_p) &= R\left(\phi, \Phi_n, \Phi_p\right),
\end{aligned}$$

subject to the boundary

$$\begin{aligned}
\left(\phi, \Phi_n, \Phi_p\right)\Big|_{\partial\Omega_D} &= \left(\phi_D, \Phi_{n,D}, \Phi_{p,D}\right),\\
\left(\frac{\partial\phi}{\partial\nu}, \frac{\partial\Phi_n}{\partial\nu}, \frac{\partial\Phi_p}{\partial\nu}\right)\Big|_{\partial\Omega_N} &= (0,0,0).
\end{aligned}$$

Markowich demonstrated the existence of weak solutions of the drift-diffusion equations with a SRH recombination proving that the map $G\left(\Phi_n^{(k)}, \Phi_p^{(k)}\right) = \left(\Phi_n^{(k+1)}, \Phi_p^{(k+1)}\right)$, defined as:

1. Given $\left(\Phi_n^{(k)}, \Phi_p^{(k)}\right)$ to solve $\phi^{(k+1)}$ in the Poisson equation

$$\varepsilon\Delta\phi^{(k+1)} = qn_i\left(\Phi_n^{(k)} e^{\frac{\phi^{(k+1)}}{U_T}} - \Phi_p^{(k)} e^{\frac{-\phi^{(k+1)}}{U_T}}\right) - qC(x), \tag{3.3.3}$$

   subject to the boundary conditions $\phi^{(k+1)}\big|_{\partial\Omega_D} = \phi_D$ and $\frac{\partial\phi^{(k+1)}}{\partial\nu}\big|_{\partial\Omega_N} = 0$

2. Solve $\Phi_n^{(k+1)}$ in the continuity equation

$$n_i U_T \nabla\cdot\left(\mu_n e^{\frac{\phi^{(k+1)}}{U_T}}\nabla\Phi_n^{(k+1)}\right) = \frac{1 - \Phi_n^{(k+1)}\Phi_p^{(k)}}{\tau_n\left(e^{\frac{\phi^{(k+1)}}{U_T}}\Phi_n^{(k)} + 1\right) + \tau_p\left(e^{\frac{-\phi^{(k+1)}}{U_T}}\Phi_p^{(k)} + 1\right)}, \tag{3.3.4}$$

subject to the boundary conditions $\Phi_n^{(k+1)}\big|_{\partial\Omega_D} = \Phi_{n,D}$ and $\frac{\partial\Phi_n^{(k+1)}}{\partial\nu}\big|_{\partial\Omega_N} = 0$

3. Solve $\Phi_p^{(k+1)}$ in the continuity equation

$$n_i U_T \nabla\left(\mu_p e^{\frac{-\phi^{(k+1)}}{U_T}} \nabla\Phi_p^{(k+1)}\right) = \frac{1 - \Phi_n^{(k)}\Phi_p^{(k+1)}}{\tau_n\left(e^{\frac{\phi^{(k+1)}}{U_T}}\Phi_n^{(k)} + 1\right) + \tau_p\left(e^{\frac{-\phi^{(k+1)}}{U_T}}\Phi_p^{(k)} + 1\right)}, \tag{3.3.5}$$

subject to the boundary conditions $\Phi_p^{(k+1)}\big|_{\partial\Omega_D} = \Phi_{p,D}$ and $\frac{\partial\Phi_p^{(k+1)}}{\partial\nu}\big|_{\partial\Omega_N} = 0$,

satisfies the conditions of the Schauder Fixed Point Theorem whenever the mobilities are bounded and the boundary conditions are smooth enough. It is important to note that the condition over the mobilities it is necessary to ensure that the differential operators in (3.3.4) and (3.3.5) let be uniformly elliptic which implies the well-posedness of map G.

For transient case,

$$\lambda^2\Delta\phi = n - p - C(x) \tag{3.3.6}$$

$$\frac{\partial n}{\partial t} = \nabla\cdot(\mu_n\nabla n - n\nabla\phi) - R(n,p) \tag{3.3.7}$$

$$\frac{\partial p}{\partial t} = \nabla\cdot\left(\mu_p\nabla p - p\nabla\phi\right) - R(n,p) \tag{3.3.8}$$

subject to the initial and boundary conditions

$$\begin{array}{llll} n(x,0) & = n_0(x) & , \quad p(x,0) & = p_0(x) \\ (\phi,n,p)\big|_{\partial\Omega_D} & = (\phi_D, n_D, p_D) & , \quad (\frac{\partial\phi}{\partial\nu}, \frac{\partial n}{\partial\nu}, \frac{\partial p}{\partial\nu})\big|_{\partial\Omega_N} & = (0,0,0) \end{array} \tag{3.3.9}$$

Gajewski, assuming that the initial conditions n_0 and p_0 are functions in $L^2(\Omega)$, the carrier mobilities are bounded functions of electric field and the Einstein is kept, demonstrated that exists a unique weak solution for short time interval by means of proving the contractivity of the map $F(n^{(k)}, p^{(k)}) = (n^{(k+1)}, p^{(k+1)})$ defined as follows, see [12] for more details:

1. Given $n^{(k)}$ and $p^{(k)}$ solve $\phi^{(k+1)}$ in the Poisson equation

$$\begin{aligned} \lambda^2\Delta\phi^{(k+1)} &= n^{(k)} - p^{(k)} - C(x) \\ \phi^{(k+1)}\big|_{\partial\Omega_D} &= \phi_D \\ \frac{\partial\phi^{(k+1)}}{\partial\nu}\big|_{\partial\Omega_N} &= 0 \end{aligned}$$

2. Solve $n^{(k+1)}$ and $p^{(k+1)}$ in the parabolic system

$$\begin{aligned}
\frac{\partial n^{(k+1)}}{\partial t} &= \nabla\cdot\left(\mu_n\nabla n^{(k+1)} - n^{(k)}\nabla\phi^{(k+1)}\right) - R(n^{(k)},p^{(k)}),\\
\frac{\partial p^{(k+1)}}{\partial t} &= \nabla\cdot\left(\mu_p\nabla p^{(k+1)} - p^{(k)}\nabla\phi^{(k+1)}\right) - R(n^{(k)},p^{(k)}),\\
\left(n^{(k+1)},p^{(k+1)}\right)\Big|_{\partial\Omega_D} &= (n_D,p_D),\\
\left(\frac{\partial n^{(k+1)}}{\partial \nu},\frac{\partial p^{(k+1)}}{\partial \nu}\right)\Big|_{\partial\Omega_N} &= (0,0).
\end{aligned}$$

It is necessary to say that the contractivity of F was proved in the set

$$M_a = \{(n,p) : \|(n,p)\| \leq a\} \tag{3.3.10}$$

where

$$\|(n,p)\| = \left[\max_{0\leq t\leq T}\left\{\|n(t)\|^2_{L^2(\Omega)} + \|p(t)\|^2_{L^2(\Omega)}\right\} + \int_0^T \left(\|n(s)\|^2_{H^1(\Omega)} + \|p(s)\|^2_{H^1(\Omega)}\right)ds\right] \tag{3.3.11}$$

Remark 3.1. The results about of existence of solutions for the drift-diffusion have been obtained for single semiconductors assuming mainly that the Einstein relation is satisfied, the carrier densities are bounded functions and that the Neumann boundary conditions are homogeneous. In the case of the model (2.3.1)-(2.3.3) boundary conditions of Robin type are impossed and existence results for this case are still an open problem.

3.3.2 Numerical methods

To study the way of improving the efficiency of the solar cell by means of the model (2.3.1)-(2.3.3), it is important to analyze the numerical methods that have been used to solve the drift-diffusion equations, such methods showed to satisfy the physical aspects and to solve certain observed mathematical difficulties.

From physical point of view is strictly necessary to implement numerical methods that conserve the carrier densities and assure their positivity also of being thermodynamically consistent. To satisfy the first two requirements non-standard discretization methods have been used in order to avoid spatial oscillations generated by small parameters obtained after the scaling of drift-diffusion equations. These small parameters convert to the drift-diffusion equations in singularly perturberd problems which are either tackled by asymptotic expansions [87, 89] or by non-standard discretization schemes, as the upwind-method [41], which are applied to adaptative meshes like Shishkin type ones [92] that are much finner when the scaling parameter is smaller.

In the case of the thermodynamical consistency, the Scharfetter-Gummel method was developed [84, 87], for the steady state case, considering a exponential behavior of charge, specifically that the carrier distributions obey the Maxwell-Boltzmann statistics (3.3.1), and approximating the potential as a piece-wise linear function for a constant field between the mesh points [43]. However, for degenerate semiconductors that obey the Fermi-Dirac statistics [93] the generalized Einstein relation should be assumed and generalizations of Scharfetter-Gummel method had to be carried out [94].

The methods that are not based on the Scharfetter-Gummel method should add correction terms to assure their thermodynamical consistency [88].

On the other hand, once the discretizations are obtained the resulting systems of nonlinear equations can be solved by Newton-type methods [95, 96] or by the Gummel method [38, 91]. The first one is widely used by its order accuracy but a suitable initial guess should be imposed, in these sense continuation methods are employed only to tackle this purpose [97]. The second one is iterative procedure of sequential type that decouples the Poisson equation by initial values of n and p for the transient case or ϕ_n and ϕ_p for the steady state case, unlike Newton' s method the Gummel method is almost unconditionally convergent but its order accuracy is less than the Newton method [90]. It is important to point out that the resulting systems are frequently badly conditioned for which preconditioners are commonly used [86]. Finally, methods based on the Schwarz domain decomposition and multigrid methods are used to deal with differential equations that are coupled in the interfaces as the case of the model (2.3.1)-(2.3.3) [30].

Remark 3.2. As we can observe to carry out numerical simulations that allow to improve the efficiency of a solar cell by means of our model different assumptions can be considered but such assumptions imply the development of suitable and novel techniques as well as great mathematical challenges.

4. Conclusions and future work

In this work a mathematical model was formulated to improve the efficiency of a single solar cell. The model is based on the drift-diffusion equations and it considers experimental parameters such as: mobility, diffusion and absorption coefficients, and doping profile among others. It takes into account phenomena as: diffusion, drift, generation and recombination of charge carriers. The model consists on three strongly coupled elliptic-parabolic systems coupled by two interfaces.

The model is applicable as for non-degenerate semiconductors as for degenerate semiconductors and allows carry out different assumptions over the parameters to improve the efficiency of the solar cell which is determined in terms of the carrier densities and the electric potential. On the other hand, the model has the limitations that the generation term does not consider different wavelengths, which are observable in time, and it does not take into account temperature variations.

After of analyzing the mathematics and physics involved in the mathematical modeling of the solar cell, this work presents the following challenges:

1. To determine the depletion region for non-uniformly distributed impurities it is necessary to find the curves γ_1 and γ_2 that delimit the regions Ω_{d_p} and Ω_{d_n} such that the charges contained in these regions are equal and satisfy the drift-diffusion equations under equilibrium conditions.

2. The boundary and interface conditions should be imposed according to the doping levels, doping profile and junction type among others and these conditions have to prove to be physically consistent.

3. To study the interfaces and the well-posedness of the model, existence and uniqueness results should be proved for elliptic-parabolic systems with Robin boundary conditions.

4. To analyze the efficiency of solar cells made from degenerate semiconductors or a combination with non-degenerate semiconductors, novel numerical methods that are thermodynamically consistent must be developed, in the case of discretization methods we want also to find a suitable technique that combines the advantages of Newton's and Gummel's methods.

5. To reproduce suitably the behavior of the carrier densities in the interfaces of the model, we have to compare the domain decomposition and multi-grid methods as well as the asymptotic expansions.

A. Semiconductor generalities

This appendix we present important aspects about the semiconductors as well as some idealizations that have been considered to model the transport of charge carriers in the semiconductors.

A.1 Semiconductor statistics

The semiconductor statistics show how are related the free and impurity carriers as well as their ionization energy. This way, the electron and hole concentrations are given by

$$n = \int_{E_c}^{\infty} D_c(E) f(E) dE, \qquad p = \int_{-\infty}^{E_v} D_v(E)(1 - f(E)) dE. \tag{A.1.1}$$

where

$$\begin{aligned} D_c(E) &= \frac{8\pi m_n \sqrt{2m_n(E - E_c)}}{h^3}, \qquad E \geq E_c \\ D_v(E) &= \frac{8\pi m_p \sqrt{2m_p(E_v - E)}}{h^3}, \qquad E \leq E_v \end{aligned}$$

are respectively the density of states in the conduction band and valence band and, m_n and m_p are respectively the effective masses of the electron and hole meanwhile h is the Planck's constant. On the other hand, $f(E)$ is a distribution function that represents the probability of a set of electronic states are occupied [103].

A.1.1 Lightly doped semiconductors

For lightly doped semiconductors also known as non-degenerate ones, the Maxwell-Boltzmann distribution

$$f_{MB}(E) = e^{-\frac{E - E_F}{kT}}, \tag{A.1.2}$$

implies that the electron and hole concentrations are

$$n = N_c e^{(E_F - E_c)/kT}, \qquad p = N_v e^{(E_v - E_F)/kT}$$

where N_c and N_v indicate respectively the effective density of states in the conduction and valence bands, given by

$$N_c = 2\left(\frac{2\pi m_n kT}{h^2}\right)^{3/2}, \qquad N_v = 2\left(\frac{2\pi m_p kT}{h^2}\right)^{3/2}$$

In thermodynamical equilibrium the law of mass action stablish that

$$np = n_i^2 = N_c N_v e^{(E_v - E_c)/kT} = N_c N_v e^{-E_g/kT}$$

where E_g represents the band gap.

A.1.2 Heavily doped semiconductors

Depending on the level of impurities and working temperatures, semiconductors have insulating or conductive properties. Lightly doped semiconductors behave as insulators at low temperatures since the impurity atoms only have the energy to move to the neighboring atom. Meanwhile, in heavily doped semiconductors the impurity atoms are at a shorter distance so a band of impurities is formed that overlaps the conduction band whereby the semiconductor acts as a conductor [104]. On the other hand, the heavily doped semiconductors obey the Fermi-Dirac distribution

$$f_{FD}(E) = \frac{1}{1 + e^{(E-E_F)/kT}}, \tag{A.1.3}$$

In the case of Fermi-Dirac distribution the integrals shown in (A.1.1) can not been explicitly determined. However, if $E \gg E_F$ then the Maxwell-Boltzmann can be used to approximated them. In any other case, the carrier densities are given by [104, 105]

$$n = N_c F_{1/2}\left(\frac{E_F - E_C}{KT}\right), \qquad p = N_v F_{1/2}\left(\frac{E_F - E_C}{KT}\right) \tag{A.1.4}$$

where

$$\mathcal{F}_\eta(x) = \int_0^\infty \frac{y^\eta}{1 + e^{y-x}} dy. \tag{A.1.5}$$

A.2 Einstein relations

The diffusion and drift processes are involved in the current density of electrons and holes and they are related as follows [107]

$$\frac{D_n}{\mu_n} = \frac{k_b T}{q}, \qquad \frac{D_p}{\mu_p} = \frac{k_b T}{q}$$

these relations as known as Einstein relations which are only valid for lightly doped semiconductors whenever as long as there is a small charge in the band edges. For degenerate semiconductors, the generalized Einstein relations for the electrons were determined by Chakravarti and Nag [108]

$$\frac{D_n}{\mu_n} \approx \frac{k_b T}{q}\left[\frac{\mathcal{F}_{1/2}(\gamma) + \frac{15\alpha k_b T}{4}\mathcal{F}_{3/2}(\gamma)}{\mathcal{F}_{-1/2}(\gamma) + \frac{15\alpha k_b T}{4}\mathcal{F}_{1/2}(\gamma)}\right] \tag{A.2.1}$$

with $\alpha \neq 0$ for non-parabolic energy bands and $\alpha = 0$ for the parabolic ones.

A.3 Ideal p-n junction

The ideal p-n junction is a idealized model in which have been impossed the following [107]:

1. n and p materials are lightly doped,
2. their respective concentrations N_D and N_A are uniformly distribuited,
3. all the dopants are ionized,
4. there is not recombination in the depletion region.

A.3.1 Carrier densities at equilibrium

Under the law of mass action $np = n_i^2$, the equilibrium hole and electron concentrations in a ideal p-n junction can be approximated by

$$p = N_A, \qquad n = \frac{n_i^2}{N_A} \tag{A.3.1}$$

in the p-region and

$$p = \frac{n_i^2}{N_D}, \qquad n = N_D \tag{A.3.2}$$

in the n-region. These concentrations are considered in the mentioned regions far from junction area [107]. On the other hand, the electrostatic potentials are given by

$$\phi_p \equiv \frac{kT}{q} \ln\left(\frac{n_i}{N_A}\right), \qquad \phi_n \equiv \frac{kT}{q} \ln\left(\frac{N_D}{n_i}\right)$$

and the built-in voltage V_{bi} is

$$V_{bi} = \phi_n + \left|\phi_p\right| = \frac{kT}{q} \ln\left(\frac{N_D N_A}{n_i^2}\right). \tag{A.3.3}$$

In addition, the width of the depletion region (W) and the maximum value of the electric field ($E_{\max}$) are given by [57]

$$W = \sqrt{\frac{2\varepsilon}{q}\left[\frac{N_A + N_D}{N_A N_D}\right] V_{bi}}, \qquad E_{max} = \frac{qN_D d_n}{\varepsilon} = \frac{qN_A d_p}{\varepsilon}$$

where

$$d_n = \sqrt{\frac{2\varepsilon}{qN_D}\left[\frac{N_A}{N_A + N_D}\right] V_{bi}}, \qquad d_p = \sqrt{\frac{2\varepsilon}{qN_A}\left[\frac{N_D}{N_A + N_D}\right] V_{bi}}.$$

A.4 Solar cell efficiency parameters

The energy conversion efficiency (η) is the relation between the generated power and the incident power (P_i) so the maximum efficiency is calculated using the formula

$$\eta = \frac{V_{max} I_{max}}{P_i} \tag{A.4.1}$$

where I_{max} and V_{max} are respectively the maximum current and voltage.

In technical terms, the efficiency of a solar cell is related with different parameters [60, 61] such as: the open circuit voltage (V_{oc}), short circuit current (I_{sc}) and the fill factor (FF) as follows

$$FF = \frac{V_{max} I_{max}}{V_{oc} I_{sc}} = \frac{\eta P_i}{V_{oc} I_{sc}}. \tag{A.4.2}$$

where I_{sc} is obtained by measuring the current in the circuit shown in Figure A.1 and V_{oc} is the potential difference between the two terminals of the cell when it is being irradiated and the current can not flow through it, it causes the electrons to be pushed to the N region and the holes to the p region, see Figure A.2.

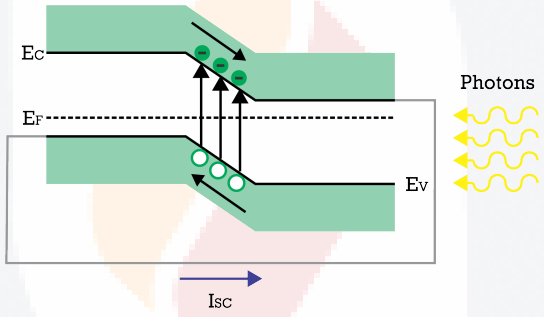

Figure A.1: Solar cell at short-circuit conditions

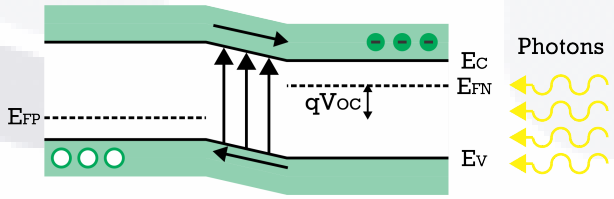

Figure A.2: Solar cell at open-circuit conditions

B. Schafetter-Gummel method

In this appendix we present the Scharfetter-Gummel method which have been widely used to numerically solve the drift-diffusion equations for non-degenerate semicondutors and for which several generalizations have been developed [84].

B.1 Assumptions over the drift-diffusion equations

Let us consider the drift-diffusion equations in one spatial dimension

$$\begin{cases} \frac{dE}{dx} = \frac{q}{\varepsilon}(p - n + N_D - N_A) \\ \frac{\partial n}{\partial t} = \frac{1}{q}\frac{\partial J_n}{\partial x} + G \\ \frac{\partial p}{\partial t} = -\frac{1}{q}\frac{\partial J_p}{\partial x} + G \end{cases} \tag{B.1.1}$$

where

$$\begin{aligned} J_n &= q\mu_n nE + kT\mu_n \frac{\partial n}{\partial x} \\ J_p &= q\mu_p pE - kT\mu_p \frac{\partial p}{\partial x} \end{aligned} \tag{B.1.2}$$

In their work, Scharfetter and Gummel [84] impossed the following assumptions over the generation-recombination rate and the carrier mobilities.

1. The generation-recombination rate G is due to two phenomena: the carrier generation and recombination through the defects denote by G_d and the ionization or avalanche ionization G_I given by

$$G_d = \frac{pn - n_i^2}{\tau_p(n + n_1) + \tau_n(p + p_1)} \tag{B.1.3}$$

and

$$G_I = \frac{1}{q}\left(\alpha_n(E)|J_n| + \alpha_p|J_p|\right) \tag{B.1.4}$$

2. The carrier mobilities are dependent of the electric field

$$\left(\frac{\mu_0}{\mu}\right)^2 = 1 + \left(\frac{N_D}{N_D/S + N}\right) + \left(\frac{(E/A)^2}{E/A + F}\right) + (E/B)^2 \tag{B.1.5}$$

where

	μ_0	N	S	A	F	B
Holes	480	$4x10^{16}$	81	$6.1x10^{3}$	1.6	$2.5x10^{4}$
Electrons	1400	$3x10^{16}$	350	$3.5x10^{3}$	8.8	$7.4x10^{3}$

Table B.1: Coefficients for the field dependent mobility

B.2 Numerical method

Due to the nonlinearities in Scharfetter-Gummel model it must be solved numerically, to achieve it, the structure is divided into small cells and the spatial derivatives in the equations are solved using standard difference approximations given by

$$\begin{cases} \dfrac{dp^{(j)}}{dt} = G^j - \dfrac{J_p^{(i)} - J_p^{(i-1)}}{\Delta x} \\ \dfrac{dn^{(j)}}{dt} = G^j + \dfrac{J_n^{(i)} - J_n^{(i-1)}}{\Delta x} \\ \dfrac{E^{(i)} - E^{(i-1)}}{\Delta x} = \frac{q}{\varepsilon}(p^{(j)} - n^{(j)} + N_D^{(j)} - N_A^{(j)}) \end{cases},$$

where the point i is at the middle of the points $j+1$ and j, then, J_n, J_p, μ_n,μ_p and E are assumed constant between mesh points, leading to the solution

$$\begin{aligned} J_p^{(i)} &= E^{(i)} \left[\frac{p^{(j)}\mu_p^{(i)}}{1 - exp(-E^{(i)}\Delta x)} + \frac{p^{(j+1)}\mu_p^{(i)}}{1 - exp(E^{(i)}\Delta x)} \right] \\ J_n^{(i)} &= E^{(i)} \left[\frac{n^{(j+1)}\mu_n^{(i)}}{1 - exp(-E^{(i)}\Delta x)} + \frac{n^{(j)}\mu_n^{(i)}}{1 - exp(E^{(i)}\Delta x)} \right] \end{aligned},$$

which is numerically stable.

For the time advancement, the equation system represented using a vector is

$$\dot{y} = f(y),$$

with y_0 and $\delta y(t)$ as the initial value of y and its time increases, respectively. Therefore

$$y(t) = y_0 + \delta y(t),$$

which for small deviations δy, $f(y)$ is expanded as

$$\delta y = f(y_0) + M\delta y,$$

where M indicates the matrix df/dy.

In the case that M, f, and δy were ordinary numbers

$$\delta y(t) = \left(e^{Mt} - 1\right) f/M, \quad \text{or } \delta y(t) = f \cdot t\left(1 + Mt/2 + (Mt)^2/6 + ...\right).$$

Additionally, in the case of small and finite time steps, the solution is given by

$$\left(1 - \frac{Mt}{2}\right)\delta y(t) = f \cdot t,$$

representing the vector equation that must be solved for each time increment which is added to y_0.

In this particular case,

$$y^j = \left\{ \begin{array}{c} \Delta n^{(j)} \\ \Delta p^{(j)} \\ \Delta E^{(i)} \end{array} \right\},$$

and,

$$f^j = \left(\begin{array}{c} \Delta p^{(j)} \\ \Delta n^{(j)} \end{array} \right).$$

And the vector equation to solve in each time is

$$\left[\frac{2}{t} - M^{(j)}\right] y^{(j)} = 2f_0^{(j)} + \Delta f_t,$$

with Δf_t as the change in $f^{(j)}$ at the terminals and $M^{(j)} = \dfrac{\partial f^{(j)}}{\partial y}$.

C. List of Symbols

In this appendix we present the meaning of the different symbols used in this dissertation.

B_λ	radiative recombination coefficient ($1.8 \times 10^{-15} cm^3 s^{-1}$) for Si
c	speed of light in the vacuum
C	doping profile
C_n	electron Auger recombination coefficient ($2.8 \times 10^{-31} cm^6 s^{-1}$) for Si
C_p	hole Auger recombination coefficient ($0.99 \times 10^{-31} cm^6 s^{-1}$) for Si
d_n	width of the n-region in the depletion region
d_p	width of the p-region in the depletion region
D_n	electron diffusion coefficient
D_p	hole diffusion coefficient
E	electric field
E_c	conduction band energy
E_g	band-gap energy
E_f	Fermi level energy
E_i	intrinsic Fermi level energy
E_{max}	maximum value of the electric field
E_T	trap energy
E_v	valence band energy
f	carrier distribution function
F	photon flux
$\tilde{F}$	absorbed photon flux
$\hat{F}$	photon flux in the generation term
G	electron-hole pair generation rate
h	Planck constant
I	current
I_f	intensity of monochromatic light flux
J	current density
J_n	electron current density
J_p	hole current density

k	Boltzmann constant
L_n	electron diffusion length
L_p	hole diffusion length
m_n	electron effective mass
m_p	hole effective mass
n	electron concentration
n_i	intrinsic carrier concentration
n_{eq}	electron concentration in equilibrium
N_A	acceptor impurities concentration
N_C	effective density of states in the conduction band
N_D	donor impurities concentration
N_V	effective density of states in the valence band
p	hole concentration
p_{eq}	hole concentration in equilibrium
q	elemental charge
r	reflection coefficient of the cell
R	electron-hole pair recombination rate
$R_{Auger,n}$	electron Auger recombination rate
$R_{Auger,p}$	hole Auger recombination rate
$R_{\lambda,n}$	electron radiative recombination rate
$R_{\lambda,p}$	hole radiative recombination rate
$R_{SRHj,n}$	electron defect assisted recombination rate
$R_{SRHj,p}$	hole defect assisted recombination rate
U	net rate of generation and recombination of electrons and holes
U_T	thermal voltage
V_a	polarization voltage
V_{bi}	built-in voltage
V_j	junction voltage
V_p	photogenerated voltage
w	width of the depletion region in an gradual junction
α	cell absorption coefficient of light the corresponding wavelength
γ	carrier concentration (electrons or holes)
ε	static dielectric constant of the semiconductor, in this case, silicon
λ	light's wavelength
μ_n	electron mobility
μ_p	holes mobility
ν	light's frequency
ϕ	electrostatic potential
ϕ_n	n region electrostatic potential
ϕ_p	p region electrostatic potential
ρ	electric charge density

τ	average collision time
$\tau_{Auger,n}$	electron lifetime in Auger recombination
$\tau_{Auger,p}$	hole lifetime in Auger recombination
$\tau_{\lambda,n}$	electron lifetime in radiative recombination
$\tau_{\lambda,p}$	hole lifetime in radiative recombination
τ_n	electron lifetime
τ_p	hole lifetime
$\tau_{SRH,n}$	electron lifetime in SRH recombination
$\tau_{SRH,p}$	hole lifetime in SRH recombination

Bibliography

[1] https://www.census.gov/newsroom/stories/2018/world-population.html

[2] https://datos.enerdata.net/energia-total/datos-consumo-internacional.html

[3] https://www.iea.org/statistics/

[4] C. Arancibia Bulnes & R. Best y Brown, *Energía del Sol*, Ciencia, 2010, pp. 10-17.

[5] Obra Social Caja Madrid, *Guía de la Energía Solar*, Industrias Gráficas el Instalador, S.L., Madrid, 2006.

[6] A. Blakersa, N. Zina, K. R. McIntoshb & K. Fonga, *High Efficiency Silicon Solar Cells*, Energy Procedia, 33(2013), pp. 1-10.

[7] M. Imamzai, M. Aghaei, Y. H. Md Thayoob & M. Forouzanfar, *A Review on Comparison between Traditional Silicon Solar Cells and Thin-Film CdTe Solar Cells*, Proceedings National Graduate Conference 2012, Universiti Tenaga Nasional, Putrajaya Campus, 2012.

[8] X. Pi, Q. Li, D. Li & D. Yang, *Spin-coating silicon-quantum-dot ink to improve solar cell efficiency*, Solar Energy Materials & Solar Cells, 95, 2011, pp. 2941-2945.

[9] T. G. Allen, J. Bullock, Q. Jeangros, C. Samundsett, Y. Wan, J. Cui, A. Hessler-Wyser, S. De Wolf, A. Javey & A. Cuevas, *A Low Resistance Calcium/Reduced Titania Passivated Contact for High Efficiency Crystalline Silicon Solar Cells*, Advanced Energy Materials, 7(12), 2017.

[10] L. Idoko, O. Anaya-Lara & A. McDonald, *Enhancing PV modules efficiency and power output using multi-concept cooling technique*, Energy Reports, 4, 2018, pp. 357-369.

[11] W. P. Mulligan, D. H. Rose, M. J. Cudzinovic, D. M. De Ceuster, K. R. McIntosh, D. D. Smith, & R. M. Swanson, *Manufacture of solar cells with 21% efficiency*, 19th European Photovoltaic Solar Energy Conference, 2004.

[12] Markowich P. A., Ringhofer C. A. and Schmeiser C. *Semiconductor Equations*, Springer Verlag 1990.

[13] K. Sopian, S. L. Cheow, & S. H. Zaidi, *An overview of crystalline silicon solar cell technology: Past, present, and future*, AIP Conference Proceedings 1877, 2017.

[14] C. Yu, S. Xu, J. Yao & S. Han, *Recent Advances in and New Perspectives on Crystalline Silicon Solar Cells with Carrier-Selective Passivation Contacts*, Crystals, 8(2018).

[15] Ma, T., Gu, W., Shen, L. & Li, M., *An improved and comprehensive mathematical model for solar photovoltaic modules under real operating conditions*, Solar Energy, 184, 2019, pp.292-304.

[16] Nazerian, V. & Babaei, S., *Optimization of Exponential Double-Diode Model for Photovoltaic Solar Cells Using GA-PSO Algorithm*, The Selected Papers of The First International Conference on Fundamental Research in Electrical Engineering, 2019.

[17] Louzazni, M. & Aroudam, E., *An analytical mathematical modeling to extract the parameters of solar cell from implicit equation to explicit form*, Appl. Sol. Energy, 51, 2015, pp.165-171.

[18] Acevedo-Luna, A. & Morales-Acevedo, A., *Study of validity of the single-diode model for solar cells by I–V curves parameters extraction using a simple numerical method*, Journal of Materials Science: Materials in Electronics, 29, 2018.

[19] Cheng, Y., Gamba, I., Majorana, A. & Shu, C., *Discontinuous Galerkin methods for the Boltzman-Poisson systems in semiconductor device simulations*, AIP Conference Proceedings 1333, 2011, pp. 890-895.

[20] W. Abd El-Basit, A. M. Abd El-Maksood & F. Abd El-Moniem Saad Soliman, *Mathematical Model for Photovoltaic Cells*, Leonardo Journal of Sciences, 2013, pp. 13-28.

[21] P. Singh, S. N. Singh, M. Lal & M. Husain, *Temperature dependence of I-V characteristics and performance parameters of silicon solar cell*, Solar Energy Materials & Solar Cells, 92, 2008, pp. 1611-1616.

[22] A. Durgadevi, S. Arulselvi & S.P.Natarajan, *Photovoltaic Modeling and Its Characteristics*, I Proceedings of ICETECT, 2011, pp. 469-475.

[23] Jung, T., Song, H., Ahn, H. & Kang, G., *A mathematical model for cell-to-module conversion considering mismatching solar cells and the resistance of the interconnection ribbon*, Solar Energy, 103, 2014, pp. 253-262.

[24] Unsur, V., Chen, N., & Ebong, A., *A mathematical investigation of the impact of gridline and busbar patterns on commercial silicon solar cell performance*, Journal of Computational Electronics, 2020.

[25] Makkar, A., Raheja, A., Chawla, R. & Gupta, S., *IoT Based Framework: Mathematical Modelling and Analysis of Dust Impact on Solar Panels*, 3D Research, 10, 2019.

[26] Ahsan, M., Ahmad, N. & Badar, H. M. W., *Simulation of Solar angles for maximizing Efficiency of Solar Thermal Collectors*, 3rd International Conference on Energy Conservation and Efficiency (ICECE), 2019, pp. 1-5.

[27] Gupta, M., Raj, A., Shikha, D., & Suman, D., *Efficiency Improvement Technique for Silicon Based Solar Cell Using Surface Texturing Method*, 3rd International Conference and Workshops on Recent Advances and Innovations in Engineering, 2018.

[28] X. H. Nguyen & M. P. Nguyen, *Mathematical modeling of photovoltaic cell/module/arrays with tags in Matlab/Simulink*, Nguyen and Nguyen Environ Syst Res, 4:24, 2015.

[29] P. A. Basore, *Numerical Modeling of Textured Silicon Solar Cells Using PC-1D*, IEEE TRANSACTIONS ON ELECTRON DEVICES, 37(2), 1990, pp. 337-343.

[30] Cercignani, C., Gamba, I., Jerome, J. & Shu, C., *A domain decomposition method: a simulation study*, Extended Abstracts of 1998 6th International Workshop on Computational Electronics, 1998, pp. 174-177.

[31] Carrillo, J., Gamba, I., Majorana, A. & Chi-Wang, S., *A WENO-Solver for the 1D Non-Stationary Boltzmann-Poisson System for Semiconductor Devices*, Journal of Computational Electronics, 1, 2002, pp. 365-370.

[32] Foster, J., Snaith, H., Leijtens, T. & Richardson, G., *A model for the operation of perovskite based hybrid solar cells: Formulation, analysis, and comparison to experiment*, SIAM Journal on Applied Mathematics, 74, 2014, pp. 1935-1966.

[33] Kirchartz, Thomas & Nelson, Jenny, *Device Modeling of Organic Bulk Heterojunction Solar Cells*, Topics in current chemistry, 2013.

[34] Calderón-Muñoz, Williams & Jara-Bravo, Cristian, *Hydrodynamic modeling of hot-carrier effects in a PN junction solar cell*, Acta Mechanica, 227, 2016.

[35] O. N. D. Kaushika et al., *Solar Photovoltaics*, Capital Publishing Company, India, 2018.

[36] Altermatt, P. *Models for numerical device simulations of crystalline silicon solar cells - A review*, Journal of Computational Electronics, 10, 2011, pp. 314-330.

[37] Scheer, H.C. & Wagemann, H., *Determination of diffusion length of solar cells*, Archiv f. Elektrotechnik, 66, 1983, pp. 327-334.

[38] Liu, L. & Li, G., *Modeling and simulation of organic solar cells*, IEEE Nanotechnol. Mater. Devices Conf., 2010, pp. 334-338.

[39] W. Schockley and W. T. Read , *Statistics of the recombination of holes and electrons*, Phys. Rev., 87 (1952), pp. 835-842.

[40] G.P. Agrawal and N.K. Dutta, *Recombination Mechanisms in Semiconductors*. In: Semiconductor Lasers. Springer, Boston pp. 74-146.

[41] Yuan He, Irene M. Gamba, Heung-Chan Lee, & Kui Ren, *On the Modeling and Simulation of Reaction-Transfer Dynamics in Semiconductor-Electrolyte Solar Cells*, SIAM J. Appl. Math, 75(6), 2015, pp. 2515-2539.

[42] Black, J.P., Breward, C., Howell, P.D. & Young, R., *Mathematical Modeling of Contact Resistance in Silicon Photovoltaic Cells*, SIAM Journal on Applied Mathematics, 73, 2013.

[43] U. Ravaioli, *Review of Conventional Semiconductor Device Models Based on Partial Differential Equations*, Advanced Theory of Semiconductors and Semiconductor Devices, 2012.

[44] Gamba, I., *Asymptotic behavior at the boundary of a semiconductor device in two space dimensions*, Annali di Matematica Pura ed Applicata, 163, 1993.

[45] Khelghati, A. & Baghaei, K., *Global existence and boundedness of classical solutions in a quasilinear parabolic-elliptic chemotaxis system with logistic source*, Comptes Rendus Mathematique, 353, 2015.

[46] Wang, L., Mu, C. & Zheng, P., *On a quasilinear parabolic-elliptic chemotaxis system with logistic source*, Journal of Differential Equations, 256, 2013.

[47] Zheng, J., *Boundedness of solutions to a quasilinear parabolic-elliptic Keller-Segel system with logistic source*, Journal of Differential Equations, 259, 2015, pp.120-140.

[48] D. Vasileska, S. M. Goodnick & G. Klimeck, *Computational Electronics: Semiclassical and Quantum Device Modeling and Simulation*, CRC Press, 2010.

[49] T. L. Floyd, *Electronic devices : conventional current version*, Prentice Hall, 2012.

[50] O. Perpiñán Lamigueiro, *Energía Solar Fotovoltaica*, Creative Commons, 2013.

[51] A. Sproul, *Understanding the p-n Junction*, UNSW.

[52] T. Soga, *Nanostructured Materials for Solar Energy Conversion*, Elsevier, 2006.

[53] C. Reig, *Física de la unión P-N*, Universitat de Valencia.

[54] A. Luque & S. Hegedus, *Handbook of Photovoltaic Science and Engineering*, John Wiley & Sons, 2011.

[55] A. McEvoy, L. Castaner & T. Markvart, *Solar Cells. Materials, Manufacture and Operation*, 2012.

[56] Matos, F.B. & Camacho, José, *A model for semiconductor photovoltaic (PV) solar cells: The physics of the energy conversion, from the solar spectrum to dc electric power*, International Conference on Clean Electrical Power, ICCEP '07, 2007, pp. 352-359.

[57] R. Messenger & J. Ventre, *Photovoltaic Systems Engineering*, CRC Press, 2004.

[58] R. Dalven, *INTRODUCTION TO APPLIED SOLID STATE PHYSICS*, Plenum Press, 1980.

[59] M. Lundstrom, *Solar Cells Lecture 1: Introduction to Photovoltaics*, http://nanohub.org/resources/11875, 2011.

[60] M. I. Kabir, Z. Ibarahim, K. Sopian & N. Amin, *A Review on Progress of Amorphous and Microcrystalline Silicon Thin-Film Solar Cells*, Recent Patents on Electrical Engineering, 4(2011), pp. 50-62.

[61] M. P. Barrera, *Simulación y caracterización de celdas solares multijuntura y de silicio cristalino para aplicaciones espaciales*, Ph.D. Thesis, Universidad Nacional de General San Martín.

[62] R. M. Swanson, *Approaching the 29% limit efficiency of silicon solar cells*, Conference Record of the Thirty-first IEEE Photovoltaic Specialists Conference, 2005, pp. 889-894.

[63] B. Michl, M. Rudiger, J.A. Giesecke, M. Hermle, W. Warta and M.C. Schubert, *Efficiency limiting bulk recombination in multicrystalline silicon solar cells*, Solar Energy Materials & Solar Cells, 98, 2018, pp. 441-447.

[64] Wang, Z., Zhang, H., Dou, B., Wu, W. & Zhang, G., *Numerical and experimental research of the characteristics of concentration solar cells*, Front Energy, 2019.

[65] W. W. Gärtner, *Depletion-Layer Photoeffects in Semiconductors*, Physical Review, Vol. 116, No. 1, 1959, pp. 84-87.

[66] I. N. Volovichev, J. E. Velázquez-Perez, Yu. G. Gurevich, *Transport boundary conditions for semiconductor structures*, Solid-State Electronics 52 (2008) 1703-1709.

[67] D. H. Foster, T. Costa, M. Peszynska and G. Schneider, *Multiscale modeling of solar cells with interface phenomena*, Journal of Coupled Systems and Multiscale Dynamics • March 2013

[68] B. H. Rose and H. T. Weaver, *Determination of effective surface recombination velocity and minority-carrier lifetime in high-efficiency Si solar cells*, J. Appl. Phys. 54 (1), January 1983

[69] A. Cuevas, D. Macdonald and R. A. Sinton, *Chapter III-1 - Characterization and Diagnosis of Silicon Wafers, Ingots, and Solar Cells*, Practical Handbook of Photovoltaics (Second Edition), Academic Press, pp. 1011-1044.

[70] C. C. Hu, *Modern Semiconductor Devices for Integrated Circuits*, Prentice Hall, 2009.

[71] Uprety, P., Subedi, I., Junda, M., Collins, R. & Podraza, N., *Photogenerated Carrier Transport Properties in Silicon Photovoltaics*, Nature Research Scientific Reports, 9, 2019, pp. 189-192.

[72] de Falco, C., Iacchetti, A., Binda, M., Natali, D., Sacco, R. & Verri, M., *Modeling and Simulation of Organic Solar Cells*, Mathematics in Industry, 16, 2012.

[73] S. Selberherr, *Analysis and Simulation of Semiconductor Devices*, Springer-Verlag/Wien, 1984.

[74] Green, M. A. & Keevers, M. J., *Optical properties of intrinsic silicon at 300 K*, Progress in Photovoltaics: Research and Applications, 3, 1995, pp. 189-192.

[75] Rajkanan, K. & Singh, R. & Shewchun, J., *Absorption coefficient of silicon for solar cell calculation*, Solid-State Electronics, 2, 1979, pp. 793-795.

[76] A. Nachaoui, *Iterative solution of the drift-diffusion equations*, Numerical Algorithms, 21 (1999), 323-341.

[77] C. Ringhofer & C. Schmeiser, *A Modified Gummel Method for the Basic Semiconductor Device Equations*, IEEE Transactions on Computed aided design, Vol. 7, No. 2, 1988, pp. 251-253.

[78] H.B. da Veiga , *Remarks on the Flow of Holes and Electrons in Crystalline Semiconductors. In: Sequeira A. (eds) Navier-Stokes Equations and Related Nonlinear Problems. Springer, Boston, MA*, 1995.

[79] J. Freshe & J. Naumann, *An Existence Theorem for Weak Solutions of the Basic Stationary Semiconductor Equations*, Applicable Analysis, Vol. 48, pp. 157-172.

[80] W. Fang & K. Ito , *Asymptotic behavior of the drift-diffusion semiconductor equations*, Journal of Differential Equations 123(1995), 567-587.

[81] T. Nagai & T. Ogawa, *Global Existence of Solutions to a Parabolic-Elliptic System of Drift-Diffusion Type in* $\mathbb{R}^2$, Funkcialaj Ekvacioj, 59 (2016), 67-112.

[82] S. Flores and S. Jerez, *Parabolic System Model for the Formation of Porous Silicon: Existence, Uniqueness, and Stability*, SIAM Journal in Applied Mathematics, Vol. 75(3) pp. 1047-1064.

[83] M. S. Mock, *An initial value problem from semiconductor device theory*, SIAM J. Math. Anal. Vol. 5 No. 4, August 1974.

[84] D. L. Scharfetter and H. K. Gummel, *Large-Signal Analysis of a Silicon Read Diode Oscillator*, IEEE TRANSACTIONS ON ELECTRON DEVICES 1(6) January 1969.

[85] C. den Heijer, S. J. Polak and W. H. A. Schilders, *A continuation method for the calculation or-potentials and currents in semiconductors*, Proc. NASECODE II Conf., Boole Press, Dublin, pp. 277-284.

[86] C. den Heijer, *Preconditioned iterative methods for nonsymmetric linear systems*, Proc. Int. Conf, Simulation of Semiconductor Decices and Processes, Pineridge Press, Swansca, 1984, pp. 267-285.

[87] P. Farrell, M. Patriarca, J. Fuhrmann and T. Koprucki, *Comparison of thermodynamically consistent charge carrier flux discretizations for Fermi-Dirac and Gauss-Fermi statistics*, Opt Quant Electron (2018) 50:101 https://doi.org/10.1007/s11082-018-1349-8

[88] S. J. Polak, C. den Heijer, W. H. A. Schilders and P. Markowich, *Semiconductor device modeling from the numerical point of view*, International Journal for Numerical Methods in Engineering, Vol 24, 763-838 (1987)

[89] P. A. Markowich, C. A. Ringhofcr, E. Langer and S. Selberherr, *An asymptotic analysis of single-junction semiconductor devices*, Report 2527, MRC, University of Wisconsin, 1983.

[90] J. W. Jerome, *The Role of Semiconductor Device Diameter and Energy-Band Bending in Convergence of Picard Iteration for Gummel's Map*, IEEE TRANSACTIONS ON ELECTRON DEVICES 32 (10) October 1985.

[91] H. K. Gummel, *A self-consistent iterative scheme for one-dimensional steady state transistor calculations*, IEEE Trans. El. Dec.. 11, 455-465 (1964).

[92] M. Stynes and L. Tobiska, *A finite difference analysis of a streamline diffusion method on a Shishkin mesh*, Numerical Algorithms 18 (1998) 337-360.

[93] H. Gajewski and K. Gröger, *Semiconductor equations for variable mobilities based on Boltzmann Statistics or Fermi-Dirac Statistics*, Math. Nachr. 140 (1989) 7-36.

[94] M. Kantner and T. Koprucki, *Non-isothermal Scharfetter–Gummel Scheme for Electro-Thermal Transport Simulation in Degenerate Semiconductors* Finite Volumes for Complex Applications IX-Methods, Theoretical Aspects, Examples. FVCA 2020. Springer Proceedings in Mathematics & Statistics, vol 323. Springer, Cham. $https://doi.org/10.1007/978-3-030-43651-3_14$.

[95] X. Fang, Q. Nib and M. Zeng, *A modified quasi-Newton method for nonlinear equations*, Journal of Computational and Applied Mathematics Volume 328, 15 January 2018, Pages 44-58 Journal of Computational and Applied Mathematics

[96] P. Deuflhard, *Modified Newton Method for the Solution of Ill-Conditioned Systems of Nonlinear Equations with Application to Multiple Shooting*, Numer. Math. 22, 289–315 (1974)

[97] C. den Heijer and W. C. Rheinboldt, *On steplength algorithms for a class of continuation methods*, SIAM J. Numer. Anal., 18, 925-948 (1981).

[98] Dubeyt, P. K. & Paranjape, V. V., *Open-circuit voltage of a Schottky-barrier solar cell*, Journal of Applied Physics, Vol. 48, No. 1, 1977.

[99] Sinton, R. A. & Cuevas, A. , *Contactless determination of current–voltage characteristics and minority-carrier lifetimes in semiconductors from quasi-steady-state photoconductance data*, Appl. Phys. Lett, Vol. 69, No. 17, 1996.

[100] Meyer, E. I. , *Extraction of Saturation Current and Ideality Factor from Measuring V_{oc} and I_{sc} of Photovoltaic Modules*, International Journal of Photoenergy, Vol. 2017, 2017.

[101] Cuevas, A. , *The recombination parameter J_0*, Energy Procedia, 55, 2014, pp. 53-62.

[102] Li, H.& Markowich, P., *A review of hydrodynamical models for semiconductors: asymptotic behavior*, Sociedade Brasileira de Matemática, Vol. 32, No. 3, 2001, pp. 321-342.

[103] E. F. Schubert, *Doping in III-V semiconductors*, Cambridge Studies in Semiconductor Physics and Microelectronic Engineering: 1, 1993

[104] M. Grundmann, *The Physics of Semiconductors, An Introduction Including Devices and Nanophysics*, Springer 2006 pp. 149-175.

[105] V. I. Fistul', *Heavily doped semiconductors*, Monographs in Semiconductor Physiscs, Plenum Press, 1969, pp. 37-77.

[106] W. Schockley, *The theory of P-N junctions in Semiconductors and P-N junctions Transistors*, The Bell System Technical Journal Volume: 28, Issue: 3, July 1949.

[107] M. Razeghi, *Fundamentals of Solid State Engineering*, Springer 2009, pp. 307-417.

[108] A. N. Chakravarti and B. R. Narg, *Generalized Einstein relation for degenerate semiconductors having non-parabolic energy bands*, Int. J. Electronics, 1074, Vol. 37(2), pp. 281-284.